



Article

Genome-Wide Identification, Evolution, and Expression Analysis of the Dirigent Gene Family in Cassava (*Manihot esculenta* Crantz)

Mingchao Li ^{1,2,†}, Kai Luo ^{1,2,†}, Wenke Zhang ^{1,2}, Man Liu ^{1,2}, Yunfei Zhang ³, Huling Huang ^{1,2}, Yinhua Chen ^{1,2} , Shugao Fan ^{3,*}  and Rui Zhang ^{1,2,*}

¹ School of Breeding and Multiplication, Sanya Institute of Breeding and Multiplication, Hainan University, Sanya 572025, China

² School of Tropical Agriculture and Forestry, Hainan University, Haikou 570228, China

³ School of Resources and Environmental Engineering, Ludong University, Yantai 264025, China; 18315941997@163.com

* Correspondence: fanshugao2006@126.com (S.F.); zhangrui@hainanu.edu.cn (R.Z.)

† These authors contributed equally to this work.

Abstract: Dirigent (*DIR*) genes play a pivotal role in plant development and stress adaptation. *Manihot esculenta* Crantz, commonly known as cassava, is a drought-resistant plant thriving in tropical and subtropical areas. It is extensively utilized for starch production, bioethanol, and animal feed. However, a comprehensive analysis of the *DIR* family genes remains unexplored in cassava, a crucial cash and forage crop in tropical and subtropical regions. In this study, we characterize a total of 26 cassava *DIRs* (*MeDIRs*) within the cassava genome, revealing their uneven distribution across 13 of the 18 chromosomes. Phylogenetic analysis classified these genes into four subfamilies: *DIR-a*, *DIR-b/d*, *DIR-c*, and *DIR-e*. Comparative synteny analysis with cassava and seven other plant species (*Arabidopsis thaliana*, poplar (*Populus trichocarpa*), soybean (*Glycine max*), tomato (*Solanum lycopersicum*), rice (*Oryza sativa*), maize (*Zea mays*), and wheat (*Triticum aestivum*)) provided insights into their likely evolution. We also predict protein interaction networks and identify *cis*-acting elements, elucidating the functional differences in *MeDIR* genes. Notably, *MeDIR* genes exhibited specific expression patterns across different tissues and in response to various abiotic and biotic stressors, such as pathogenic bacteria, cadmium chloride (CdCl_2), and atrazine. Further validation through quantitative real-time PCR (qRT-PCR) confirmed the response of *DIR* genes to osmotic and salt stress. These findings offer a comprehensive resource for understanding the characteristics and biological functions of *MeDIR* genes in cassava, enhancing our knowledge of plant stress adaptation mechanisms.

Keywords: cassava; forage; dirigent; gene family; phylogenetic analysis; expression pattern



Citation: Li, M.; Luo, K.; Zhang, W.; Liu, M.; Zhang, Y.; Huang, H.; Chen, Y.; Fan, S.; Zhang, R. Genome-Wide Identification, Evolution, and Expression Analysis of the Dirigent Gene Family in Cassava (*Manihot esculenta* Crantz). *Agronomy* **2024**, *14*, 1758. <https://doi.org/10.3390/agronomy14081758>

Academic Editor: Ainong Shi

Received: 8 July 2024

Revised: 3 August 2024

Accepted: 8 August 2024

Published: 11 August 2024



Copyright: © 2024 by the authors. Licensee MDPI, Basel, Switzerland. This article is an open access article distributed under the terms and conditions of the Creative Commons Attribution (CC BY) license (<https://creativecommons.org/licenses/by/4.0/>).

1. Introduction

Plants respond to environmental challenges by activating a variety of genes, including those encoding dirigent proteins (*DIR*) [1]. The role of *DIR* proteins was first discovered in Border Forsythia (*Forsythia × intermedia*) in 1997, where they were found to guide the stereoselective coupling of coniferyl alcohol (CA) radicals, leading to the production of (+)-pinoresinol, a type of lignan [2]. Pinoresinol can be converted into other lignans, such as piperitol, laciresinol, and secoisolaresinol, which have been shown to play significant roles in plant defense against pathogens [3,4]. *DIR* proteins are also implicated in the formation of lignin, with the dirigent protein model hypothesizing their regulation over the formation of specific chemical bonds during monolignol polymerization to create lignin polymers [5–8]. Additionally, techniques such as in situ mRNA hybridization and immunolabeling have revealed that *DIRs* related to lignin synthesis are primarily localized

in the secondary cell wall and other lignification tissues [5,9]. This indicates that DIR proteins not only catalyze the polymerization of monolignol (coniferyl alcohol) to form lignans but also share a partial biosynthetic pathway with lignan and lignin. Lignans can be transported to the plant cytoderm, where they are converted into lignin. DIR proteins are part of a relatively conserved multi-gene family, characterized by a significant conserved domain that constitutes a large portion of the protein. Usually, the *DIR* genes do not contain introns [10]. Ralph et al. [1] reported that *DIR* family genes can be classified into seven groups, designated as DIR-a to DIR-g, based on their evolutionary relationships. The expansion of DIR proteins has led to the identification of two additional subfamilies, DIR-f and DIR-g, with the DIR-b and DIR-d subfamilies being clustered together [11]. Biochemical experiments have demonstrated that the DIR-a subfamily members can direct the polymerization of monolignols into their proper 3D structure, while the biological roles of members of other DIR subfamily remain unknown. As a result, subfamilies other than DIR-a are often referred to as DIR-like [2,12–14]. Recently, the *DIR* gene family has been characterized on a genome-wide scale in several plant species, including pepper (*Capsicum annuum*) [15], rice [16,17], and potato (*Solanum tuberosum*) [18].

The functions of numerous plant DIR proteins have been elucidated. The DIR-a subfamily members are involved in the synthesis of pinoresinol [1,10]. Several DIRb/d subfamily members are involved in aromatic diterpenoid biosynthesis [19,20] and pterocarpan biosynthesis [21,22], while the DIR-e subfamily is believed to play a role in the formation of Casparian band lignin [23]. Additionally, *DIR* genes have been implicated in plant responses to abiotic and biotic stresses. For instance, transcripts of *BhDIR1* have been observed to respond to various exogenous hormones and abiotic stresses, such as ethylene glycol tetraacetic acid (EGTA), abscisic acid (ABA), dehydration, temperature, calcium chloride, and hydrogen peroxide stresses [24]. The loss of function of *CaDIR7* in pepper weakened plant defense against both mannitol-induced and sodium chloride (NaCl) stress [15]. The overexpression of *OsDIR55* improves the development of root apoplastic diffusion barriers and enhances salt tolerance by restricting the rise of Na⁺ concentrations and the Na⁺/K⁺ ratio [25]. Among the 37 *DIR* and *DIR-like* genes of mungbean (*Vigna radiata*), 24 genes are up-regulated by salinity [26]. Lignin acts as a non-degradable mechanical barrier, making the host plant less susceptible to many microorganisms [27]. In canola, the constitutive expression of the *DIR* gene observed increased resistance to a broad spectrum of fungal pathogens [28]. The overexpression of *GHDIR1* in cotton (*Nicotiana tabacum*) conferred resistance to the spread of *Verticillium dahlia* [29]. Similar results were found in wheat [14], soybean [30], peppers [15], and flax (*Linum usitatissimum*) [10].

Cassava, a vital staple crop in tropical and subtropical regions, serves as a primary food source for over 700 million people worldwide [31]. Its foliage boasts a high protein content (ranging from 16.41% to 22.68%), along with essential minerals and gross energy [32,33]. In many countries, cassava foliage is utilized as animal feed, showing promise in enhancing livestock production [34,35]. Notably, cassava foliage harvests exhibit seasonality, with greater biomass availability during summer or rainy seasons [35]. Despite its significance as a cash and forage crop, our understanding of *DIR* family members in cassava remains limited. Given that *DIR* genes are involved in regulating various important physiological processes, it is highly important to systematically investigate *DIR* family members in cassava. With the release of the whole-genome sequence of cassava [32], we have an opportunity to systematically investigate the evolutionary traits, organization, and expression profiles of the *DIR* gene family members in cassava at the genome-wide level. In this study, a total of 26 cassava *DIR* (*MeDIR*) genes were identified from the genome of cassava. Additionally, we conducted a comprehensive bioinformatic analysis of the *MeDIR* genes. We also performed global expression analyses to identify the involvement of specific *MeDIR* genes in various tissues and under different stress conditions. Moreover, the expression patterns in cassava in response to osmotic (polyethylene glycol, PEG) and salt (NaCl solution) stressors were examined using qRT-PCR. This study offers valuable insights into the evolutionary history and functional characterization of *MeDIR* genes in cassava.

2. Materials and Methods

2.1. Identification and General Characterization Analysis of MeDIR Members in Cassava

To identify DIR family members in cassava, we first obtained the corresponding genomic DNA sequences, coding DNA sequences (CDs), and other related sequences from EnsemblPlants (European Molecular Biology Laboratory's European Bioinformatics Institute, Cambridge, London, UK) (<http://plants.ensembl.org/index.html>, accessed on 1 April 2024). We employed the Hidden Markov Model (HMM) profile for DIR-specific domains (PF03018), as defined by the Pfam database (<http://pfam.xfam.org/family>, accessed on 1 April 2024), as queries [36]. The queries were used to search against the cassava proteome database using HMM3.4 software, setting an *E*-value of < 0.001 [37]. Further, DIR protein sequences from Arabidopsis [11] and rice [16], downloaded from Uniprot (<https://www.uniprot.org/>, accessed on 1 April 2024), EMBL-EBI, PIR, and the SIB Swiss Institute of Bioinformatics, April 2024) and Phytozome v13 (<https://phytozome-next.jgi.doe.gov/>, accessed on 3 April 2024, Energy's Joint Genome Institute), respectively, served as queries in a BLAST search for cassava DIR proteins using TBtools v2.096 software (South China Agricultural University) [38]. Candidate proteins were retained for further analysis if they contained known conserved domains via the Conserved Domain Database (CDD) (<https://www.ncbi.nlm.nih.gov/cdd/>, accessed on 3 April 2024, National Center for Biotechnology Information of the National Library of Medicine, National Institutes of Health) [39] and InterProScan (<https://www.ebi.ac.uk/interpro/>, accessed on 3 April 2024, EMBL-EBI) [40]. This method was similarly applied to identify DIR protein sequences in poplar. The physicochemical properties of the MeDIR proteins were estimated using the ExPASy tool (<https://web.expasy.org/protparam/>, accessed on 6 April 2024, SIB Swiss Institute of Bioinformatics) [41]. Furthermore, the subcellular localization of MeDIR protein sequences was predicted using the WoLF PSORT online tool (<https://wolfpsort.hgc.jp/>, accessed on 9 April 2024, developers: Paul HORTON and Keun-Joon PARK at CBRC, Takeshi OBAYASHI, and Kenta NAKAI) [42].

2.2. Sequence Analysis and Structural Characterization

Gene structures were analyzed using the Gene Structure Display Server (GSDS: <http://gsds.cbi.pku.edu.cn>, accessed on 10 April 2024) [43]. The exon/intron structure was determined by comparing the genomic DNA and CDS sequences of *MeDIR* genes. The MEME online software v5.5.6 (<https://meme-suite.org/meme/>, accessed on 10 April 2024, University of Nevada, Reno, NV, USA) was utilized to analyze the protein sequences with the following parameters: the maximum number of motifs was set to ten, with all others settings at default. Identified motifs were annotated according to InterProScan (<http://www.ebi.ac.uk/Tools/pfa/iprscan/>, accessed on 10 April 2024, EMBL-EBI). Sequence logos for *MeDIR* were created using the WebLogo website (<http://weblogo.berkeley.edu/logo.cgi>, accessed on 10 April 2024, Computational Genomics Research Group, Department of Plant and Microbial Biology, University of California, Berkeley, CA, USA) [44]. The Gene Structure View module in TBtools v2.096 was used to visualize the motifs and domains of *MeDIR* genes [38].

2.3. Phylogenetic Analysis

To investigate the phylogenetic relationships of MeDIR proteins, the protein sequences of DIR proteins in cassava, Arabidopsis, rice, and poplar were aligned using Clustal W software v2.1 (Kyoto University Bioinformatics Center, Kyoto, Japan) under default parameters [45]. A phylogenetic tree was generated using the neighbor-joining (NJ) method with 1000 bootstrap replications in MEGA v7.1 software and visualized with the EvolView v3 online tool (<https://www.evolgenius.info/>, accessed on 15 April 2024) [46].

2.4. Secondary Structure Prediction and Three-Dimensional (3D) Model Construction

The secondary structure of the deduced polypeptides was predicted using SOPMA (https://npsa.lyon.inserm.fr/cgi-bin/npsa_automat.pl?page=/NPSA/npsa_sopma.html,

accessed on 15 April 2024, Pôle Rhône-Alpes de Bio-Informatique). The tertiary structure of MeDIR proteins was predicted using Phyre2 with intensive modeling. Phyre2 (<http://www.sbg.bio.ic.ac.uk/phyre2/html/page.cgi?id=index>, accessed on 15 April 2024, Structural Bioinformatics Group, Imperial College, London, UK) was also employed to search for MeDIR homologs using the amino acid sequences as target sequences.

2.5. Chromosomal Localization and Gene Duplication

MeDIR genes were mapped onto cassava chromosomes by identifying their position in genome version 6.1 from the Phytozome v13 database (<https://phytozome.jgi.doe.gov/>, 18 April 2024) and visualized by Tbtools v2.096 [38]. Collinear blocks were evaluated by MCScan2 (<https://github.com/wyp1125/MCScanX>, accessed on 18 April 2024), considering alignments with an E -value $\leq 1 \times 10^{-10}$ as significant matches [47]. The syntenic relationship between MeDIR genes was determined and displayed using TBtools v2.096 software [38]. The Ka/Ks (non-synonymous substitution rate/synonymous substitution rate) values were calculated to analyze the selection pressure and selection mode after identifying duplicate genes.

2.6. Analysis of Promoter Regions

The 2000 bp upstream DNA sequence of MeDIRs, considered the promoter region, was retrieved from the Phytozome v13 database. The PlantCARE online program (<http://bioinformatics.psb.ugent.be/webtools/plantcare/html/>, accessed on 20 April 2024, joint lab at University of Pretoria) [48] was used to predict *cis*-regulatory elements in the promoter regions of MeDIR genes, and TBtools v2.096 was employed to visualize the results [38].

2.7. Protein Interaction Network Diagram and GO Annotation

Interologues of Arabidopsis were used to predict the protein–protein interaction network for MeDIRs using the STRING v12.0 protein interaction database (<http://string-db.org/>, accessed on 25 April 2024, EMBL-EBI, CPR, and the SIB Swiss Institute of Bioinformatics), with the confidence parameter set at 0.15 [49,50]. GO enrichment analysis, including the molecular function (MF), biological process (BP), and cellular component (CC), was performed using Pannzer2 (<http://ekhidna2.biocenter.helsinki.fi/sansspanz/>, accessed on 26 April 2024, University of Helsinki Institute of Life Sciences, Helsinki, Finland). All Amino acid sequences were submitted in fasta format. GO terms were annotated using Bioinformatics (<http://www.bioinformatics.com.cn/>, accessed on 28 April 2024, Chinese Academy of Sciences, Beijing, China, Shanghai Jiaotong University, Shanghai, China, Xiangya School of Medicine, Changsha).

2.8. RNA-Seq Data Analysis

The transcriptome data retrieved from the NCBI database (accession numbers: PRJNA324539, GEO dataset: GSE82279, and cassava variety: TME204) [51] were used to analyze the global expression of MeDIR genes in various cassava tissues. Another set of data about cassava bacterial blight (*Xanthomonas phaseoli* pv. *manihotis* str. *Xam668*) (accession numbers: PRJNA163523, strain origin: Indonesia) [52] was used to investigate the expression profiles of MeDIR genes in response to pathogen invasion. Transcriptome data for CdCl₂ [accession numbers: PRJNA1128429, cassava variety: South China 9 (SC9)] and atrazine stress (accession numbers: PRJNA1127687, cassava variety: SC9) were obtained from our group. Subsequently, Log₂ Fold Change (Log₂ FC) values were calculated to evaluate gene expression using TBtools v2.096 software [38].

2.9. Plant Materials and Osmotic and Salt Stress Treatments

SC9, a typical cassava cultivar derived from the National Cassava Germplasm Nursery, was used. The SC9 stem segments were planted in 1/2 strength Hoagland nutrient solution medium and grown in a greenhouse at Hainan University (Haikou, Hainan, China) under controlled conditions for about 40 days and watered every three days before being subjected

to osmotic and salt stress treatments. Seedlings were treated with 1/2 strength Hoagland nutrient solution medium with 20% polyethylene glycol (PEG) 6000 and 400 mM NaCl for 4, 12, and 24 h [53,54], respectively, for the osmotic and salt stress treatments. Untreated seedlings (0 h) served as controls. Samples were immediately frozen in liquid nitrogen for RNA isolation.

2.10. RNA Isolation and qRT-PCR

RNA was isolated from leaves using the RNAPrep Pure Plan Plus Kit (TIANGEN Biotech Co., Ltd., Beijing, China) according to the manufacturer's instructions. Total RNA (1 µg) was used for first-strand cDNA synthesis with a reverse transcriptase kit (M1631, Thermo Fisher Scientific, Waltham, MA, USA). The elongation factor 1 α (EF1 α) gene served as an internal control. Primers listed in Table S1 were utilized. Real-time PCR was conducted on a 7500 Real-Time PCR System (Thermo Fisher Scientific) with a 20 µL total reaction volume, containing 2 µL cDNA template, 1 µL forward primer, 1 µL reverse primer, 10 µL qPCR Master Mix, and 6 µL sterilized ddH₂O. The amplification protocol was set as follows: 95 °C for 30 s for 40 cycles, 95 °C for 5 s, 55 °C for 30 s, 72 °C for 30 s, and a final extension at 72 °C for 10 min [55]. Each reaction was performed in triplicate. Relative gene expression levels were calculated using the $2^{-\Delta\Delta CT}$ method [56]. The significance analysis was conducted by using the ANOVA in IBM SPSS Statistics v26 software (International Business Machines Corporation, Armonk, NY, USA). Multiple tests were performed using the Duncan method through variance analysis of different comparison groups.

3. Results

3.1. Identification and Characterization of MeDIRs in Cassava Genome

A total of 26 MeDIR proteins in cassava were identified through stringent bioinformatics analyses (Table S2), with all subsequently undergoing domain analysis using CDD and InterProScan. This confirmed the presence of the conserved DIR domain (PF03018). Based on their chromosome locations, these cassava DIR genes were renamed from *MeDIR1* to *MeDIR26*. The ExPASy online tool facilitated the analysis of the physical and chemical characteristics of the MeDIR proteins (Table S2).

The CDs of the MeDIRs ranged from 399 bp to 1119 bp, encoding peptides of 132 to 372 amino acids. The MW of these peptides varied from 14.44 to 38.48 kDa, with *pI* ranging from 4.25 to 9.84. Additionally, the GRAVY index of MeDIR proteins varied from -0.176 to 0.289 , the instability index ranged from 19.31 to 43.13, and the fatty acid index ranged from 66.72 to 106.49. The subcellular localizations of MeDIRs, predicted using the WoLF PSORT web service, revealed that 13 MeDIR proteins were located in the chloroplast, 5 in the extracellular space, 4 in the cytoskeleton, 2 in the endoplasmic reticulum, 1 in the nucleolus, and 1 in the vacuole (Table S2). Pairwise sequence similarities among the predicted amino acids of the 26 MeDIRs showed a variation in identity from as low as 15.88% (*MeDIR3* vs. *MeDIR13*) to as high as 100% (*MeDIR2* vs. *MeDIR26*) (Table S3). Four pairs of genes (*MeDIR2* vs. *MeDIR26*, *MeDIR2* vs. *MeDIR6*, *MeDIR6* vs. *MeDIR26*, *MeDIR19* vs. *MeDIR15*), sharing an amino acid identity greater than 91%, may represent alleles within the species.

3.2. Secondary and Tertiary Structures and Homologs of MeDIRs

The SOPMA online program was utilized to predict the structural features of 26 MeDIR proteins, aiming to better understand their molecular functions (Table S4). The analysis revealed that the random coil configuration constituted a significant portion of the MeDIR proteins' secondary structures, ranging from 35.64% to 63.44%. The fraction of the beta turn was less than 9% of the overall structure. The alpha helix and extended strand structure comprised 11.11–25.26% and 22.04–40.15% of the secondary structures, respectively.

The predicted three-dimensional structures for the 26 MeDIR proteins are illustrated in Figure 1. Each query sequence matched four top-scoring proteins. Notably, the hypothetical protein c4revB identified as a disease resistance response protein 206 (drr206) and three other proteins belonging to the allene oxide cyclase-like protein (AOC) family were found.

The c4revB shared 25–72% sequence identity with MeDIRs and was predicted as a homolog of DIR with 100% probability. The AOC barrel-like protein d2brja1 exhibited 18–25% sequence identity with MeDIRs, with a probability of being a DIR homolog of 97.3–98.3%. The probabilities for the other two proteins, d1zvca1 and c4h69A, were estimated at 96.8–98.3% and 96.7–98.2%, respectively (Table S5).

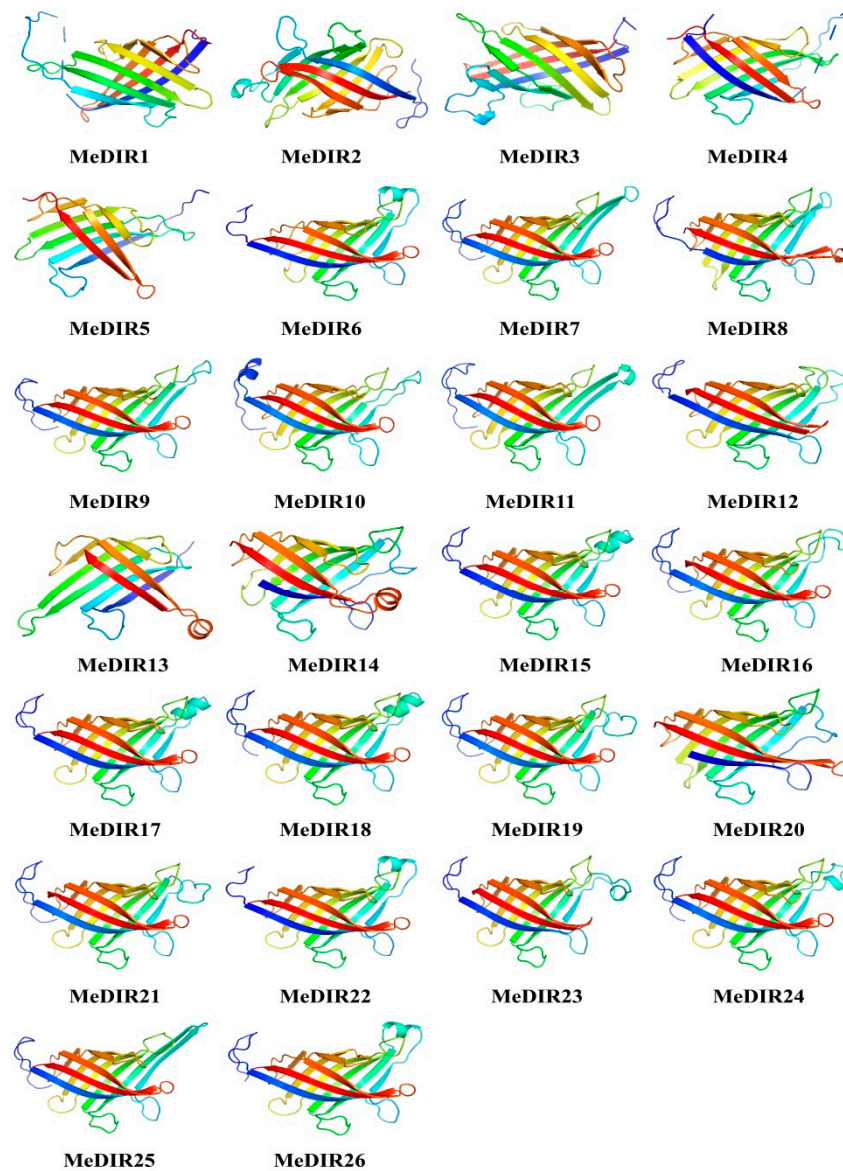


Figure 1. Prediction of the three-dimensional structure of MeDIR proteins. The colors indicate the predicted confidence of the model along the sequence. Blue indicates the minimum confidence and red indicates the highest confidence.

3.3. Phylogenetic Relationship Analysis

A phylogenetic analysis was conducted to investigate the relationships and evolutionary history within the MeDIR family, incorporating 139 *DIR* and *DIR-like* gene protein sequences from Arabidopsis, rice, and poplar as reference proteins. Based on the classification of Ralph et al. [11], the phylogenetic tree was divided into four distinct subfamilies: DIR-a, DIR-b/d, DIR-c, and DIR-e. The DIR-a subfamily, an ancient and conserved clade, included 4 *MeDIRs*, 5 *AtDIRs* (Arabidopsis *DIRs*), 7 *OsDIRs* (rice *DIRs*), and 11 *PtDIRs* (poplar *DIRs*). The DIR-b/d subfamily was the largest, comprising 15 *MeDIRs*, 14 *AtDIRs*, 11 *OsDIRs*, and 16 *PtDIRs*, indicating considerable expansion in cassava. The DIR-c subfamily contained only 13 *OsDIRs*, suggesting a monocotyledon-specific expansion. As

previously reported, the DIR-a family members are capable of directing the *in vitro* stereoselective formation of lignans, so the members of this group are known as dirigent genes [11]. Meanwhile, the members of the DIR-b/d, DIR-c, DIR-d, DIR-e, and DIR-g subfamilies are referred to as dirigent-like genes [1,11]. Thus, *MeDIR1*, *MeDIR3*, *MeDIR4*, and *MeDIR5* are classified as dirigent genes, whereas the remaining 22 *MeDIR* genes are considered *DIR-like* genes. A separate phylogenetic analysis exclusive to *MeDIR* genes demonstrated that genes within each group clustered together, reinforcing their categorized relationships (Figure 2).

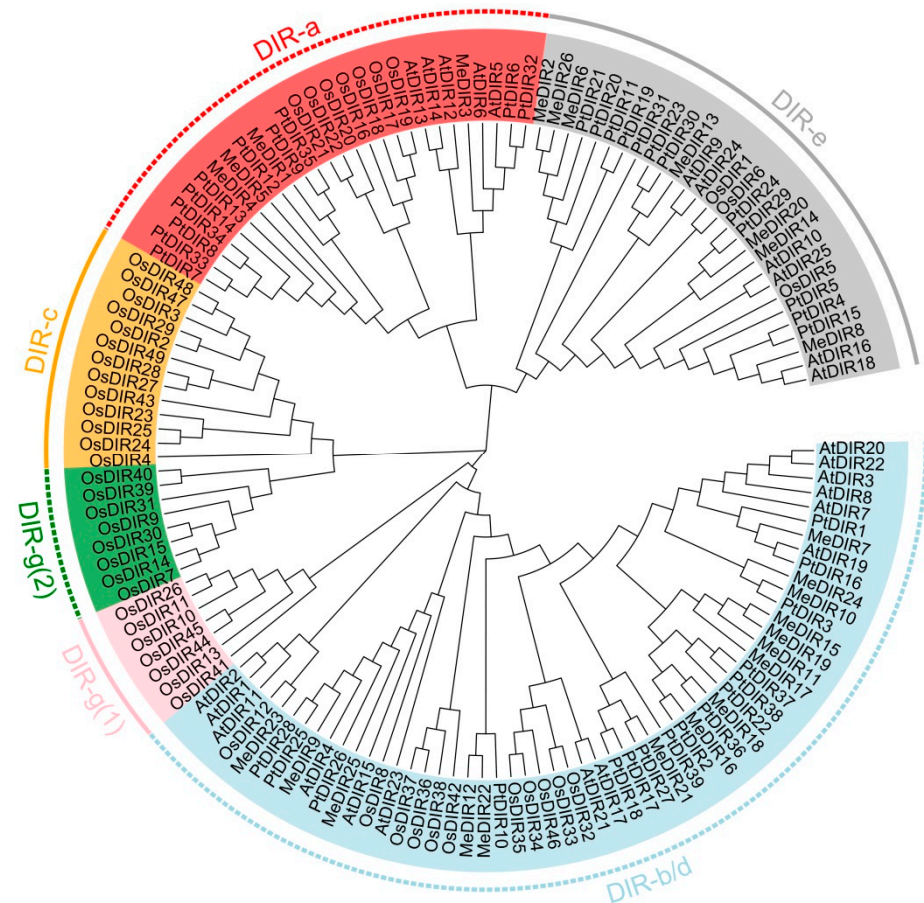


Figure 2. Phylogenetic tree of the DIR proteins predicted in cassava and those previously identified in Arabidopsis, rice, and poplar. The phylogenetic tree was constructed using the Neighbor-joining (NJ) method with 1000 bootstrap replications as implemented in MEGA7.1 from a DIR protein sequence alignment. Different clades are distinguished by different colors. Me, *Manihot esculanta*; At, *Arabidopsis thaliana*; Os, *Oryza sativa*; Pt, *Populus trichocarpa*.

3.4. Chromosomal Locations, Duplication Events, and Synteny Analysis

To investigate the genomic distribution of the cassava *DIR* genes, we mapped their chromosomal locations on the cassava plant genome's pseudochromosome assembly to identify duplicated blocks. The analysis revealed that the 26 *MeDIR* genes are unevenly distributed across 13 of cassava's 18 chromosomes (Table S2; Figure 3A). Among these chromosomes, chromosome 2 harbors the highest number of *MeDIR* genes, totaling four members. Chromosomes 4, 8, and 15 each contain three genes, whereas chromosomes 1, 3, 7, and 9 have two genes each. The remaining chromosomes 6, 10, 11, 13, and 17 each possess one *MeDIR* gene.

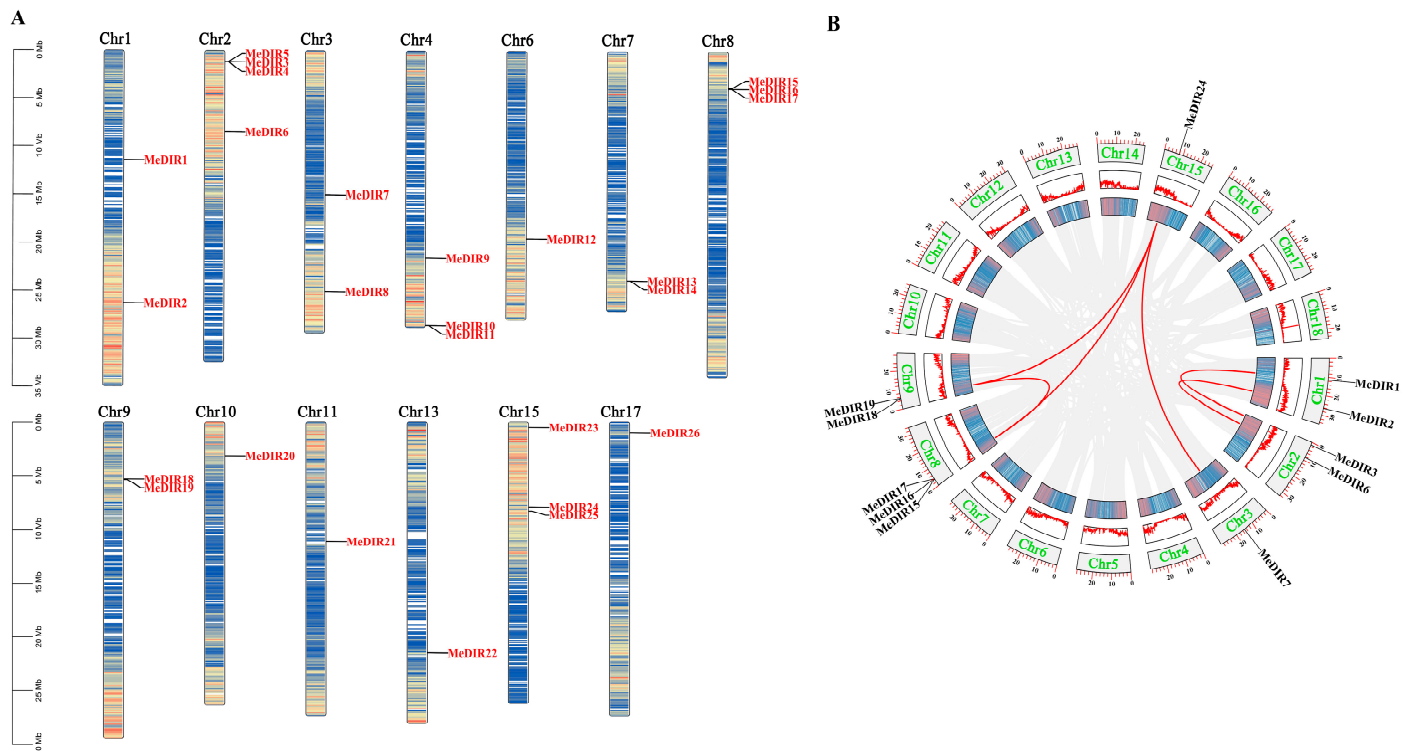


Figure 3. Mapping and synteny analysis of *MeDIR* genes. **(A)** Distribution of *DIR* genes on cassava chromosomes. The chromosome numbers were shown at the left of each chromosome. The genes were listed on the left of the chromosomes. The scale on the left is in million bases (Mb). Yellow to blue represents chromosome gene density from high to low. **(B)** CIRCOS figure of *MeDIR* genes. The gray line in the background indicates a collinear block in the genome of cassava, while the red line highlights the isomorphous gene pair. The positions of *MeDIR15* and *MeDIR16*, and *MeDIR18* and *MeDIR19* genes are very close to each other, and the lines of the two gene pairs *MeDIR15* and *MeDIR19*, and *MeDIR16* and *MeDIR18* appear to be highly overlapped. The chromosome number is indicated in each chromosome. The number of each chromosome is indicated inside each bar. The scale above the box is in mega bases (Mb). The line and heat map in the outer circle represent gene density on the chromosome. The innermost circle, from pink to blue, represents chromosomes from high to low, followed by the red bar graph, where the high and low of the bar graph represent the high and low of the chromosome density.

Tandem and segmental duplications within the cassava genome were explored using MCScanX 2 software, identifying seven segmental duplication pairs among the *MeDIR* genes (Figure 3B). These findings imply that gene duplication events, particularly segmental duplication events, have significantly contributed to the evolution of the *MeDIR* genes. To further examine the selective pressure acting on these duplicated gene pairs, we calculated the K_a and K_s substitution ratios (K_a/K_s). The K_a/K_s ratios for cassava *MeDIR* gene pairs were all below 1 (Table S6), suggesting that they evolved under the purifying selection. A comparative analysis with other species, including both dicots (*Arabidopsis*, soybean, tomato, and poplar) and monocots (rice, wheat, and maize), provides a valuable reference for understanding genetic relationships and gene functions across species. This analysis identified 14, 19, 16, 25, 4, 6, and 3 pairs of homologous genes in *Arabidopsis*, soybean, tomato, poplar, rice, wheat, and maize, respectively (Figure 4).



Figure 4. Synteny analysis of *DIR* genes between cassava and seven other plant species. The gray lines in the background indicate all synteny blocks within the cassava and the other genomes, and red lines indicate the duplicated *DIR* gene pairs.

3.5. Motifs, Conserved Domains, and Gene Structure in MeDIRs

Phylogenetic analysis, restricted to *MeDIR* family members from the cassava genome (Figure 5A), unveiled a structure similar to the one derived from comparing *DIR* sequences across four plant species shown in Figure 2. Utilizing the MEME online program, we identified ten conserved motifs shared by the *MeDIR* proteins, thereby highlighting their diversity within cassava (Figure 5B). The details of the putative motifs are shown in Figure S1. Notably, motif 2, found in all *MeDIR* proteins, likely represents the conserved *DIR* domain (Figure 5C). For instance, motif 8 only exists in *MeDIR1*, *MeDIR3*, *MeDIR4*, and *MeDIR5*, and motif 9 exists only in *MeDIR13*, *MeDIR14*, and *MeDIR20*, suggesting functional diversification among *MeDIR* proteins. Additionally, proteins within the same

group exhibited similar motifs, illustrating divergence across different groups. Exon–intron composition analysis revealed that 24 of the 26 identified *MeDIR* genes comprise one exon without any introns, which is consistent with the classical *DIR* gene structure [16]. The exception is *MeDIR3* and *MeDIR17*, which had one and two exons, respectively (Figure 5D).

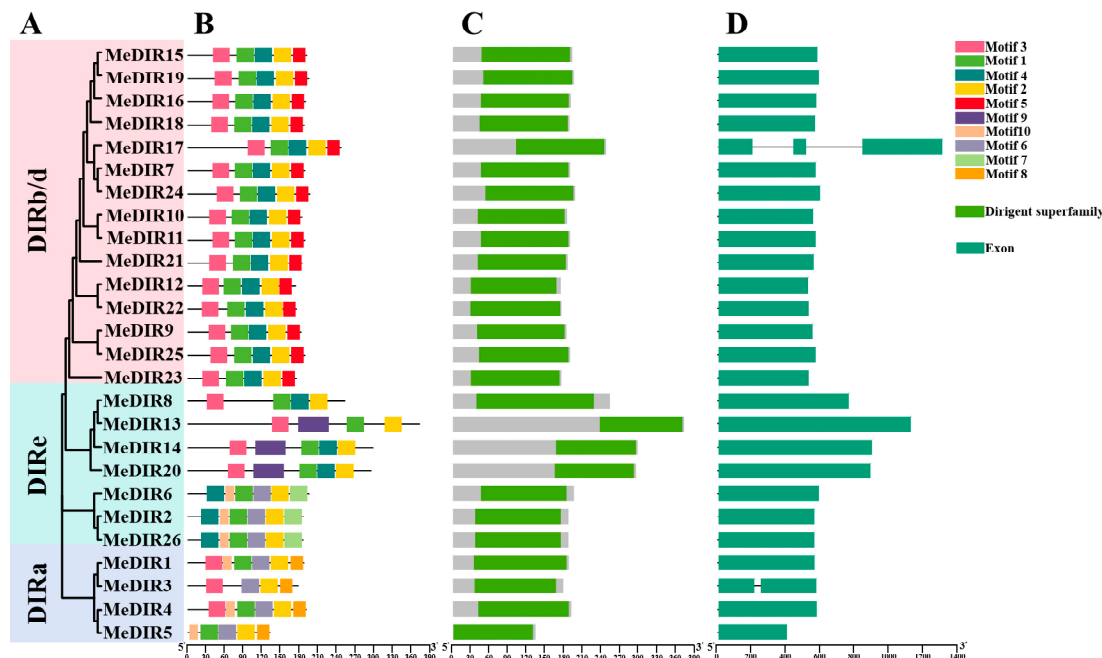


Figure 5. Phylogenetic relationships, conserved motifs, conserved domains, and gene structure of the predicted cassava DIR proteins. (A) The phylogenetic tree of cassava DIR proteins was constructed using the Neighbor-joining (NJ) method in MEGA 7.1 software, and the bootstrap value of the main branches was set to 1000 replicates. The genes in seven subgroups are marked with different colors. (B) Different motif compositions of cassava DIR proteins were detected using MEME. The boxes with different colors on the right denote 10 motifs. (C) Conserved domain in the cassava DIR proteins, where light green boxes represent domain. (D) Gene structure in the cassava DIR proteins, where bottle green boxes represent exons while black lines represent introns.

3.6. Analysis of Cis-Elements in the Promoters of *MeDIR* Family Genes

To determine the specific types and distribution of *cis*-acting elements present in the promoters of *MeDIR* family genes, an analysis of promoter *cis*-acting elements was conducted using PlantCARE. From the predicted results, a total of 29 representative *cis*-acting elements were identified within the 2.0 kb upstream region of the 26 *MeDIR* genes, highlighting an uneven distribution (Figure 6A, Table S7). Among these, light-responsive regulatory elements were predominant, with eight different types detected across nearly all *MeDIR* promoters (Figure 6A, Table S7). Hormone response *cis*-elements spanned seven categories, encompassing responses to auxin (AuxRR-core and TGA-element), gibberellin (P-box and TATC-box), abscisic acid (ABRE), methyl jasmonate (CGTCA-motif), and salicylic acid (TCA-element). Additionally, six stress-responsive elements (TC-rich repeats, W box, LTR, ARE, WUN-motif, and MBS) were identified (Figure 6A). Each of the 26 *MeDIR* genes featured at least one stress-responsive element, and all except *MeDIR9* and *MeDIR23* harbored at least one hormone-responsive element. *MeDIR15* is expected to have the highest number of *cis*-elements (Figure 6B). These results indicate that the expanded *MeDIRs* could be significantly involved in hormone signaling as well as the mechanism of stress adaptation in cassava. Furthermore, eight elements associated with tissue-specific expression were identified in *MeDIR* promoters, including RY-element, CAT-box, GCN4_motif, HD-Zip 1, O₂-site, MBSI, GC-motif, and MSA-like, hinting at their involvement in plant

growth and development. This comprehensive analysis of *MeDIR* gene family promoters significantly enriches our understanding of their intricate biological functions.

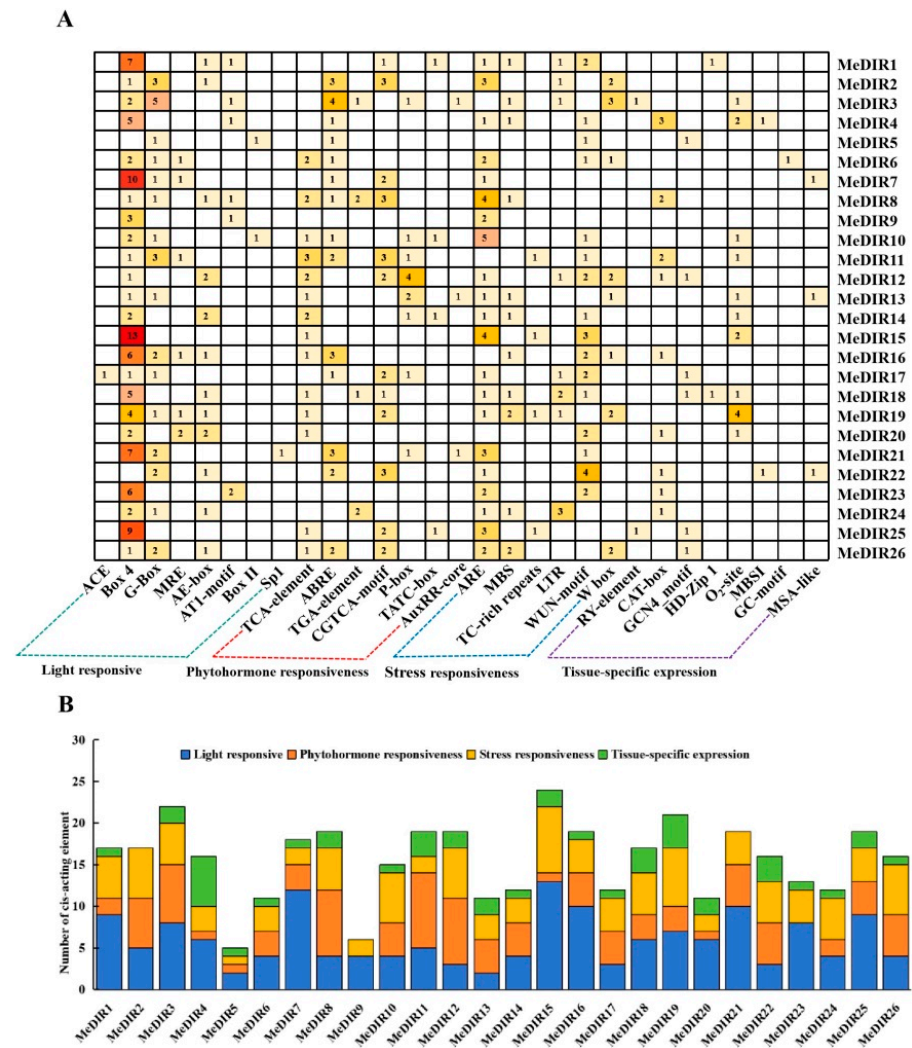


Figure 6. Analysis of *cis*-acting elements in *MeDIR* genes. (A) The grid displays various colors and numbers to represent the quantities of *cis*-acting elements present in each *MeDIR* gene. Light orange to red indicates more to less. See Table S7 for details (B) The various colors displayed on the histograms correspond to the cumulative total of *cis*-acting elements within each category.

3.7. Protein–Protein Interaction Network and GO Annotation Analysis of *MeDIRs*

Utilizing the STRING database and insights from studies on *AtDIR* and gene homology, we constructed a protein–protein interaction network for *MeDIR* proteins (Figure 7). Our analysis revealed 21 *DIR* functional molecules (*DIR*1-2, *DIR*4, *DIR*5, *DIR*6, *DIR*8, *DIR*9, *DIR*10, *DIR*11, *DIR*12, *DIR*13, *DIR*14, *DIR*16, *DIR*17, *DIR*18, *DIR*19, *DIR*20, *DIR*21, *DIR*22, *DIR*23, *DIR*24, and *DIR*25) and two putative interaction proteins (*MXA*21.17 and *NAC*057), statistically linked to 26 *MeDIR* proteins (Figure 7).

GO functional analysis delineated the BP, MF, and CC characteristics of the *MeDIR* proteins (Table S8). This analysis revealed their putative molecular and biological functions. In the “biological process” category, most proteins were classified as involved in the phenylpropanoid biosynthetic process (GO:0009699), and only one gene was classified as involved in the jasmonic acid biosynthetic process (GO:0009695). In the “molecular function” category, only one gene was classified as having allene-oxide cyclase activity (GO:0046423). Two GO terms related to cellular components, namely apoplast (GO:0048046)

and membrane (GO:0016020), were notably enriched. These results indicate that MeDIR proteins are involved in diverse aspects of cellular metabolism.

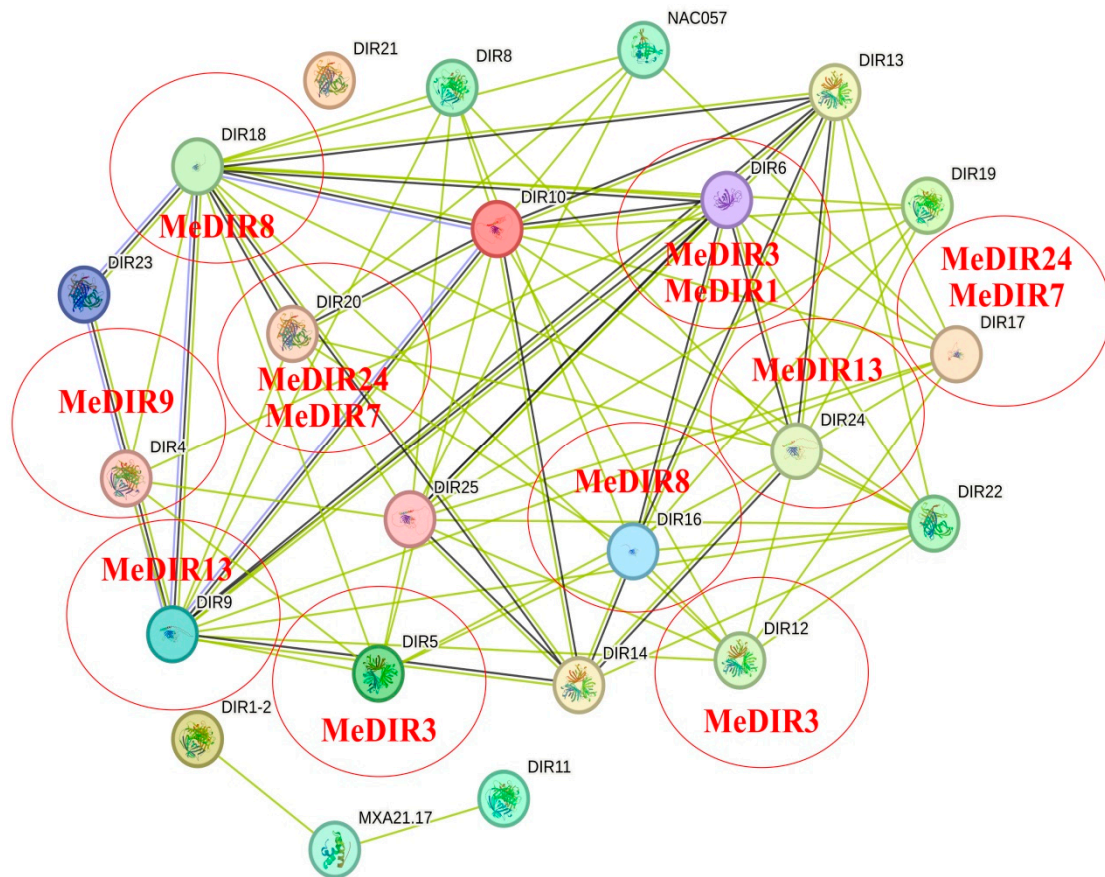


Figure 7. Protein–protein interaction network of MeDIR proteins based on their orthologs in Arabidopsis. The color scales represent the relative signal intensity scores. Colored nodes: query proteins and first shell of interactors; white nodes: second shell of interactors; filled nodes: some 3D structure is known or predicted.

3.8. Expression of MeDIR Genes in Different Tissues

Employing publicly available cassava RNA-seq data from Wilson et al. [51], we assessed the expression profiles of MeDIR genes across eleven distinct tissues: friable embryogenic callus (FEC), organized embryogenic structures (OES), fibrous root (FR), lateral buds, shoot apical meristem (SAM), petiole, root apical meristem (RAM), leaf, stem, midvein, and storage root (SR). Hierarchical clustering analysis, encompassing all 26 MeDIR genes (Figure 8), unveiled diverse expression patterns across cassava tissues. Notably, MeDIR7 and MeDIR5 were more prominently expressed across nearly all tissues, hinting at their important roles in cassava development. Certain MeDIR genes displayed tissue-specific expression patterns. MeDIR2, MeDIR12, and MeDIR24 were most expressed in fibrous roots (FR). MeDIR1, MeDIR4, MeDIR18, MeDIR23, and MeDIR24 showed elevated levels in RAM. MeDIR1 was most expressed in the stem and petiole. The expression levels of MeDIR4 and MeDIR19 were the highest in OES and SAM, respectively. These patterns of high expression in specific tissues suggest crucial roles in tissue development or functionality (Figure 8).

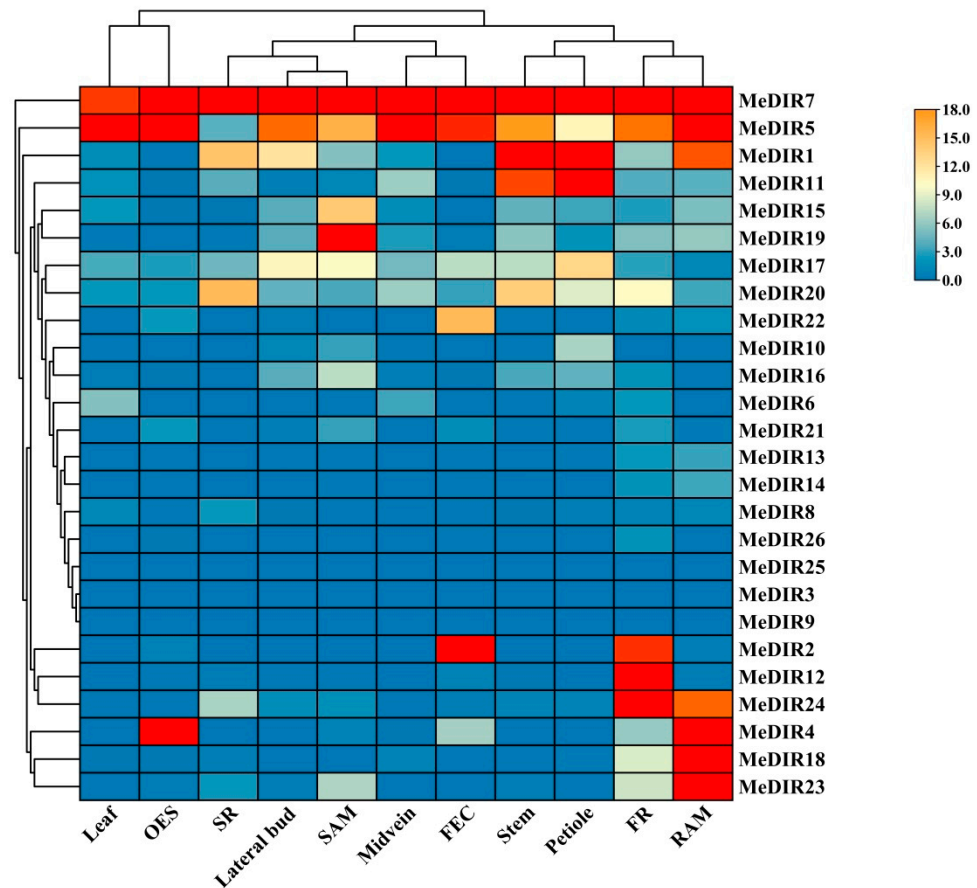


Figure 8. The expression patterns of *MeDIR* genes in different cassava tissues. The color gradient from red to blue represents varying levels of gene expression, with red indicating high expression and blue indicating low expression. FEC, OES, FR, SAM, RAM, and SR represent friable embryogenic callus, organized embryogenic structures, fibrous root, shoot apical meristem, root apical meristem, and storage root, respectively. Log₂ transformed FPKM value was used to create the heat map. The scale represents the relative signal intensity of FPKM values.

3.9. Expression Profile of *MeDIR* Genes in Response to Pathogen Infection, CdCl₂, and Atrazine Treatments

According to the cassava RNA-seq data from our group, we investigated the expression patterns of *MeDIR* genes following *Xam668* infection, CdCl₂ exposure, and atrazine treatment. All 26 *MeDIR* genes were included in the hierarchical clustering analysis. Our results demonstrated that nearly all *DIR* genes were induced by *Xam668* infection (Figure S1). Specifically, the expression of *MeDIR1*, *MeDIR12*, *MeDIR18*, and *MeDIR24* increased significantly at 8 h post-infection (hpi). *MeDIR9* and *MeDIR18* were markedly inhibited at 24 hpi. Additionally, *MeDIR16* exhibited reduced expression at 8 and 24 hpi, followed by a substantial increase at 50 hpi under *Xam668* infection. The expression levels of *MeDIR1*, *MeDIR4*, *MeDIR6*, *MeDIR7*, and *MeDIR11* increased significantly at 24 hpi. Notably, certain cassava *MeDIR* family genes, such as *MeDIR1* and *MeDIR10*, were consistently up-regulated following infection, indicating that these genes may play key roles in regulating common signaling pathways in response to *Xam668* infection.

Under atrazine stress, *MeDIR* family genes exhibited generally higher expression in leaves compared to roots. Seventeen of them (*MeDIR1*, *MeDIR2*, *MeDIR6*, *MeDIR7*, *MeDIR8*, *MeDIR10*, *MeDIR11*, *MeDIR14*, *MeDIR15*, *MeDIR16*, *MeDIR17*, *MeDIR18*, *MeDIR19*, *MeDIR20*, *MeDIR22*, *MeDIR23*, and *MeDIR26*) exhibited differential expression patterns when the leaves were stressed by atrazine for 7 days, with *MeDIR2* displaying the most significant expression trend (Figure S2). After 14 days of atrazine stress, 12 *MeDIR* genes were down-regulated, with *MeDIR2*, *MeDIR6*, *MeDIR10*, *MeDIR18*, and *MeDIR22* showing

consistent down-regulation at both time points. *MeDIR3*, *MeDIR9*, and *MeDIR25* were not expressed at any time point under atrazine stress. Most *MeDIR* genes were down-regulated in the root. In total, twenty-three *DIR* genes exhibited differential expression patterns in cassava roots following atrazine stress, with 17 genes down-regulated after 7 days and 19 genes down-regulated after 14 days. *MeDIR12* was significantly up-regulated after 7 days of stress, whereas *MeDIR15* was most significantly down-regulated after 14 days of stress.

Following CdCl_2 treatment, the expression of *MeDIR1*, *MeDIR11*, and *MeDIR15* in leaves increased significantly under low-concentration (10 $\mu\text{mol/L}$ CdCl_2 , T10) CdCl_2 stress but was promptly reduced under high-concentration (100 $\mu\text{mol/L}$ CdCl_2 , T100) CdCl_2 stress (Figure S3). The expression levels of *MeDIR20* and *MeDIR24* in T100 were significantly higher than in the control and T10 treatments. *MeDIR8*, *MeDIR12*, *MeDIR22*, and *MeDIR24* in leaves exhibited an initial decrease followed by an increase. In leaves, *MeDIR1*, *MeDIR11*, *MeDIR15*, *MeDIR17*, and *MeDIR19* exhibited a comparable expression pattern, characterized by a sharp increase following T10, followed by a decline after T100. Under T10 CdCl_2 stress, three *DIR* genes (*MeDIR1*, *MeDIR11*, and *MeDIR15*) were differentially expressed and up-regulated. Six *DIR* genes (*MeDIR4*, *MeDIR5*, *MeDIR9*, *MeDIR13*, *MeDIR14*, and *MeDIR25*) were not expressed under either cadmium concentration. *MeDIR24* was significantly activated under high concentrations (T100) of CdCl_2 .

3.10. Expression of *MeDIR* Genes under PEG and NaCl Stresses

To identify *DIR* genes in the cassava genome that respond to osmotic and salt stress, RNA was extracted from cassava seedlings' leaves subjected to salt and osmotic stress, and the relative expression levels of 20 *MeDIR* family members were assessed using qRT-PCR. For 16 out of these genes, expression levels consistently increased in response to osmotic stress (Figure 9). Among them, eleven genes (*MeDIR1*, *MeDIR2*, *MeDIR8*, *MeDIR12*, *MeDIR15*, *MeDIR17*, *MeDIR20*, *MeDIR21*, *MeDIR22*, *MeDIR24*, and *MeDIR26*) displayed heightened expression, with *MeDIR2* showing the highest level. In contrast, *MeDIR3* and *MeDIR25* exhibited significantly lower expression levels compared to the control. Six *DIR* genes (*MeDIR1*, *MeDIR11*, *MeDIR20*, *MeDIR22*, *MeDIR24*, and *MeDIR26*) were progressively suppressed, with their expression down-regulated at 24 h compared to 12 h. The expression of 14 genes (*MeDIR1*, *MeDIR2*, *MeDIR4*, *MeDIR6*, *MeDIR7*, *MeDIR8*, *MeDIR14*, *MeDIR15*, *MeDIR17*, *MeDIR19*, *MeDIR20*, *MeDIR21*, *MeDIR24*, and *MeDIR26*) reached a maximum value after 4 h of stress.

In comparison to osmotic stress, the *MeDIR* gene family exhibited greater abundance under salt stress treatment (Figure 10). Following NaCl treatment, the expression of *MeDIR1*, *MeDIR2*, *MeDIR4*, *MeDIR7*, *MeDIR11*, *MeDIR12*, *MeDIR15*, *MeDIR18*, *MeDIR20*, *MeDIR22*, *MeDIR24*, and *MeDIR26* increased considerably and peaked at 12 h. *MeDIR7*, *MeDIR20*, and *MeDIR22* demonstrated notably higher expression levels in response to salt stress compared to other genes. The expression levels of *MeDIR3*, *MeDIR19*, *MeDIR21*, and *MeDIR25* increased significantly and reached their maximum value at 24 h. Interestingly, some cassava *DIR* genes, including *MeDIR2*, *MeDIR8*, *MeDIR12*, *MeDIR15*, *MeDIR21*, *MeDIR22*, and *MeDIR26*, were consistently up-regulated across various stress conditions. This suggests that these cassava *DIR* family members may be involved in regulating common signaling pathways that manage different stress responses.

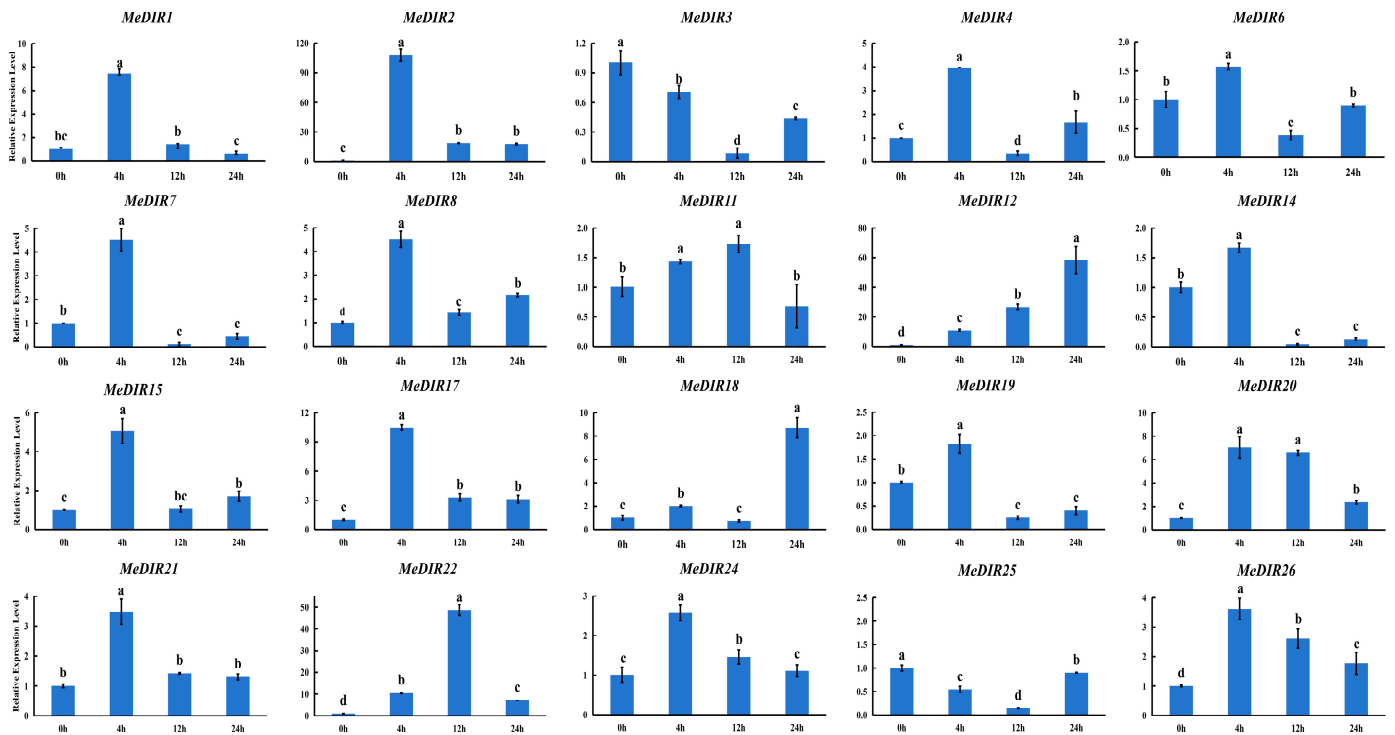


Figure 9. Expression profiles of *MeDIR* genes under PEG treatment in cassava as determined by qRT-PCR. The error bars represent the standard error of the means of three independent replicates. Values represented by the same letter showed no significant difference at $p < 0.05$ based on Duncan's multiple-range tests.

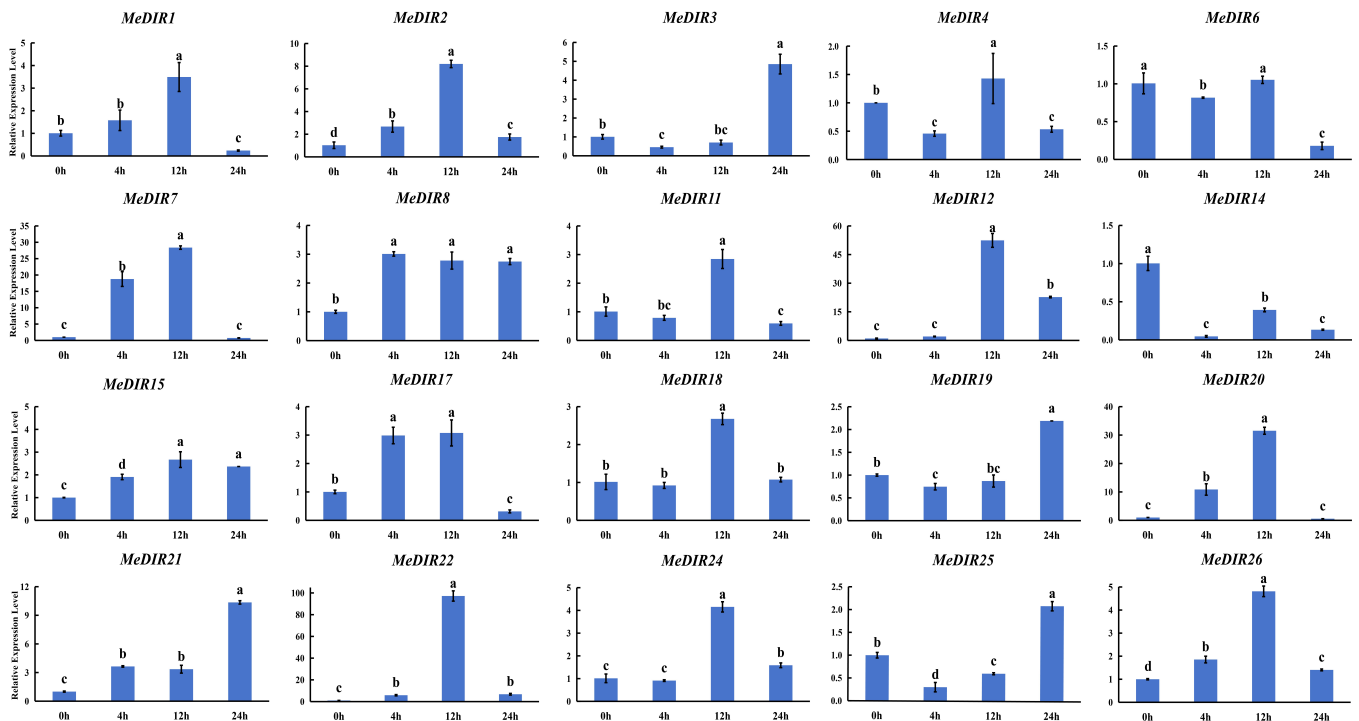


Figure 10. Expression profiles of *MeDIR* genes under NaCl treatment in cassava as determined by qRT-PCR. The error bars represent the standard error of the means of three independent replicates. Values represented by the same letter showed no significant difference at $p < 0.05$ based on Duncan's multiple-range tests.

4. Discussion

DIR and DIR-like proteins are part of a widespread multi-gene family found in most terrestrial plants. They are believed to have evolved key enzymatic functions for the synthesis of lignin and lignan, crucial for plants' adaptation from aquatic to terrestrial habitats [9,13]. In plants, the *DIR* gene family not only plays a pivotal role in the synthesis of structural polymers but also significantly impacts plant growth, development, stress responses, and secondary metabolic processes [10,15,28–30,57], making them crucial in molecular breeding for enhanced biotic and abiotic resistance. Lignin is a widespread biopolymer in plants, playing a crucial role in the structure of plant cell walls [58,59]. In cassava, the *DIR* gene family is significantly linked to lignin synthesis, alongside other gene families such as *MePOD*, *MeRAV*, *MeCAD*, and *MePAL*. The *MePOD12* gene can mitigate excess reactive oxygen species during the initial stages of postharvest physiological deterioration (PPD) and contribute to lignin deposition through its interaction with *MeCAD15*, thereby postponing PPD onset [58]. Additionally, *MeRAV5* interacts with both *MePOD* and *MeCAD* (including *MeCAD5*, *MeCAD14*, and *MeCAD15*), enhancing cassava's drought tolerance by aiding in the removal of hydrogen peroxide and lignin production [59]. According to Yao et al. [60], the *PAL* gene boosts lignin synthesis in response to the two-spotted spider mite infestation, which is crucial for plant defense against piercing and sucking herbivores and offers potential genes for developing pest-resistant cassava varieties through molecular breeding. These cassava genes are vital for improving resistance to diseases, drought, and insect pests, as well as supporting plant growth. Previous studies have established the functional roles of several subtribe *DIR* genes, with the DIR-a subfamily being involved in pinosresinol biosynthesis [1,10]. Some members of the DIR-b/d subfamily are associated with the production of aromatic diterpenoids [19,20] and pterocarpan [21,22], while the DIR-e subfamily is thought to play a role in forming Casparian strip lignin [23]. However, a comprehensive genome-wide analysis of *DIR* family genes in cassava has not yet been conducted. Extensive characterization of *DIR* family genes has been conducted in various higher plants; 25 in *Arabidopsis* [11], 24 in pepper [15], 35 in spruce (*Picea* spp.) [11], 45 in alfalfa (*Medicago sativa*) [61], 54 in rice [16], and 54 in soybean [57]. Despite the critical economic and nutritional role of cassava as a dual-purpose crop (tuber and forage), little was known about the expression and function of the *DIR* gene family before our study. Using HMMER search and BLASTp methods, we identified 26 *DIR* proteins within the cassava genome, distributed across 13 out of 18 chromosomes. These proteins vary in amino acid length from 132 a.a. (*MeDIR5*) to 372 a.a. (*MeDIR13*), with the DIR-e subfamily members exhibiting the longest sequences, and MW ranging from 14.44 (*MeDIR5*) to 38.48 kDa (*MeDIR13*). This indicates that as plants have evolved and their environments have changed over time, their divergence has led to structural variations among species [62]. Subcellular localization studies have indicated that the majority of cassava *DIR* proteins are located in the chloroplast, suggesting a specialized role in managing a variety of tasks [63,64]. The 26 *MeDIR* proteins had a *pI* ranging from 4.25 (*MeDIR13*) to 9.84 (*MeDIR7*) and most had *pI* > 7, indicating that this gene family tends to be enriched in basic amino acids.

DIR genes in cassava were clearly classified into four subfamilies: DIR-a, DIR-b/d, DIR-c, and DIR-e. This classification and the topological structure of genes align with those reported in previous studies [16,65,66], confirming the conserved nature of these subfamilies across different species. Notably, our phylogenetic analysis revealed that certain cassava *DIR* genes were included in the same clusters as the members from *Arabidopsis*, suggesting that these genes may not only share a common ancestral *DIR* gene but also retain similar biological functions, which are crucial for their roles in plant physiology and defense mechanisms [1]. Notably, the DIR-a and DIR-g subfamilies are found only in rice, indicating a distant relationship to cassava and suggesting limited homology between cassava and monocotyledonous plants like rice. This suggests a high degree of conservation among different plant species, implying that homologous genes may exhibit similar functions across species. For example, *MeDIR1*, *MeDIR3*, *MeDIR4*, and *MeDIR5*, which are closely related to drought, salt, osmotic, trauma, and oxidative stress response genes *AtDIR5* [67],

may also produce similar stress responses in cassava. Similarly, *AtDIR19* and *AtDIR7* in response to heat stress may also have similar functions to the cassava *DIR* genes belonging to the DIRb/d subfamily.

Although the physicochemical properties of the cassava *DIR* family, such as protein length, MW, and pI, were highly variable, the gene structure and amino acid motifs were relatively conserved. The findings indicate that the various descriptions of the *DIR* gene structure are interconnected, with the results highlighting the distinct characteristics of this gene family. The prediction of the tertiary structure and domain analysis of *MeDIR* genes together underscore their high level of conservation. Combined with the gene structure and conserved protein motif analysis of *MeDIR* family members, we found that members of the same subfamily have similar gene structures and conserved motif distributions among themselves, while different subfamilies have larger differences, suggesting conservation within the same subfamily and similar functions, which is consistent with the results of Zhang et al. [67] and Jia et al. [18]. The majority of cassava *DIR* family genes exhibit a simple genomic structure, predominantly consisting of one exon, which is consistent with the exon/intron structures of *DIR* genes in other diverse plants such as rice [16], potato [18], pepper [15], strawberry (*Fragaria ananassa*) [68], watermelon (*Citrullus lanatus*), cucumber (*Cucumis sativus*) [69] and pear (*Pyrus* spp.) [70]. This structural simplicity suggests a possible evolutionary advantage in maintaining a streamlined gene architecture for rapid gene expression. Additionally, the expansion of the *DIR* gene family in cassava has been influenced by segmental duplication, reflecting a common evolutionary strategy among plants to adapt and diversify their genomic capabilities [71].

Gene duplication is a pivotal mechanism that drives the evolution and diversification of gene families across species. Our analysis of gene duplication events in the 26 *MeDIR* genes identified seven pairs of segmentally duplicated genes, indicating that the expansion of the cassava *DIR* family is primarily due to segmental duplications. These findings suggest that both segmental and tandem duplications have played a significant role in the growth of the *DIR* gene family in cassava. Segmental and tandem duplication has also occurred in *DIR* genes of other species. In the duplication analysis of *CaDIRs* in capsicum, ten clusters of segmental duplication and two pairs of tandem duplication events were found [15]. Similar duplication events have been reported in the *DIR* gene families of rice [16]. Interestingly, the K_a/K_s ratios for these gene pairs were found to be less than one, suggesting that the duplicated *MeDIR* genes are predominantly under purifying selection pressure after gene duplications. Similar duplication events have been noted in other plants [15,16,70,72–75]. Furthermore, synteny analysis revealed a significant number of orthologous gene pairs between cassava and four other dicots, while fewer orthologues were observed with three monocots. This difference may be due to the evolutionary divergence between monocots and dicots over extended periods of natural selection. The phylogenetic analysis also supports this finding, showing that cassava is more closely related to dicots than to monocots.

Gene promoter analysis is essential for unraveling the complex regulatory architecture that governs gene expression [74]. The presence of *cis*-elements in gene promoter regions plays a crucial role in regulating transcription, as these elements respond to a range of environmental and developmental signals [75,76]. In cassava *MeDIR* genes, *cis*-elements associated with light responsiveness were predominant, constituting 38% of the total identified *cis*-elements, followed by elements responsive to phytohormones and biotic and abiotic stresses. The functional differentiation of *DIR* genes has been revealed at the gene expression level in different plant tissues. It has been reported that the expression of most *OsDIR* genes is comparatively higher in roots, shoot apical meristem, and panicle development than in seed development and leaves, implying that *OsDIR* genes play an important role in the development of these tissues [16]. In pepper, *CaDIRs* showed the highest expression in flowers, followed by the stem, leaf, green fruit, and red fruit, with the lowest expression levels in roots [15]. Most cassava *DIR* genes displayed relatively higher expression levels in the fibrous root (FR) and root apical meristem (RAM) and

lower expression levels in the friable embryogenic callus (FEC) and lateral bud, suggesting specific functions in diverse tissues and developmental stages. Furthermore, we found that *MeDIR5* and *MeDIR7* were expressed at high levels in all tissues, suggesting that these genes may play important roles in the growth process of cassava. The expression patterns of *DIR* genes in cassava varied across different tissues, indicating that the expression patterns of *MeDIR* family members exhibit tissue specificity. Gene expression profiling indicates that the *MeDIR* gene family may play a crucial role in regulating cassava growth and development, with *MeDIR5* and *MeDIR7* being particularly significant. The involvement of the *DIR* gene family in both biotic and abiotic stresses is well-documented across various plant species. Khan et al. [15] found that *CaDIR7* plays an important role in the defense response of pepper to *Phytophthora capsici* infection. Ralph et al. [1] showed that spruce *DIR* genes play a role in both ongoing and induced phenolic defense response mechanisms against stem-boring insects. Likewise, *TaDIR2* in wheat [77] and *GbDIR18* in cotton [65] have been linked to resistance against fungal diseases. Moreover, the deposition of lignin is regarded as an effective physical barrier against pathogen invasion [78]. Thus, similar roles are observed in defense against pathogens. For instance, in Arabidopsis, specific *DIR* genes like *AtDIR5* and *AtDIR22* regulate pathogen resistance through the salicylic acid (SA)-signaling pathway [8]. Based on transcriptomic data, *DIR* gene expression was differentially expressed after Xam668 infection. Notably, *MeDIR1* and *MeDIR10* expression increased at all three time points, indicating its potential role in cassava's defense response to Xam668 infection. Following low and high concentrations of CdCl₂ stress, *MeDIR2*, *MeDIR6*, *MeDIR22*, and *MeDIR26* were all down-regulated. Overall, there were significantly more differentially expressed genes in roots than in leaves under atrazine stress, while *DIR* genes were generally more expressed in leaves than in roots. Both *MeDIR2*, *MeDIR6*, *MeDIR10*, *MeDIR18*, and *MeDIR22* were down-regulated in atrazine-treated leaves at 7 and 14 days, while *MeDIR17* was consistently up-regulated. The majority of *MeDIR* genes exhibited down-regulation in the roots.

Previous studies have confirmed that *DIR* expression responds to salt and osmotic stress [8,15,79]. Research shows that mungbean *DIR* genes vary in their responses under these conditions [26]. Gou et al. [80] found that NaCl and PEG treatment induced *ScDIR* gene expression. Similarly, the transcript levels of *CaDIR4*, *CaDIR7*, and *CaDIR12* were significantly altered in capsicum under NaCl or mannitol stress [15]. Gong et al. [81] found that the expression levels of *SiDIR10*, *SiDIR19*, *SiDIR20*, *SiDIR22*, *SiDIR27*, and *SiDIR36* could be induced by NaCl treatment, suggesting their potential roles in coping with salt stress. In this study, we employed qRT-PCR to ascertain the expression levels of *MeDIR* genes under osmotic and salt stress conditions. Specifically, *MeDIR2*, *MeDIR8*, *MeDIR12*, *MeDIR15*, *MeDIR21*, *MeDIR22*, and *MeDIR26* demonstrated consistent up-regulation, while *MeDIR25* showed consistent down-regulation in response to treatments with PEG and NaCl. This indicates their roles in key signaling pathways mediating stress responses. The presence of stress-responsive and tissue-specific elements within *DIR* genes is likely associated with their favorable responses to biotic and abiotic stresses, as observed in gene expression profiles. In particular, most *MeDIR* genes contain ABRE elements, which are extensively involved in the ABA pathway in response to NaCl stress [82]. Correspondingly, *MeDIR* genes were found to be extensively and significantly upregulated under NaCl stress in qRT-PCR analysis. In summary, the varying expression patterns of *DIR* genes under biotic and abiotic stresses suggest a complex response mechanism within this gene family. Consequently, further investigation into the specific functions of these genes in relation to biotic and abiotic stress is warranted, as it could offer new insights into plant stress responses. The *DIR* genes exhibit positive responses to salt and osmotic stress, indicating their potential as valuable genetic resources for enhancing plant tolerance in challenging environments.

5. Conclusions

In this study, we systematically identified 26 *MeDIR* genes from the entire cassava genome and categorized them into six subfamilies. Members of each subfamily shared similar gene structures, with some *MeDIR* genes resulting from gene duplication events. Despite significant variations in the physicochemical properties of the *MeDIR* family, the gene structures and conserved protein sequences were highly conserved. The 26 *MeDIR* genes were randomly distributed across thirteen chromosomes and were subject to purifying selection. The promoter regions of *MeDIR* genes contained *cis*-acting elements associated with plant growth and development, environmental stress responses, and hormone responses. Notably, all 26 *DIR* genes had hormone response elements, along with tissue-specific expression elements, suggesting a crucial role for *MeDIR* genes in cassava growth and development as well as hormone signal transduction. Analysis of existing cassava transcriptome data revealed distinct expression profiles of *DIR* genes across various tissues, indicating potential divergent roles in cassava development. The varied expression patterns of the *MeDIR* family in different tissues suggest their involvement in responding to both abiotic and biotic stresses. Specifically, under NaCl and osmotic stress treatments, *MeDIR* genes were strongly upregulated, indicating a role in cassava's adaptation to these conditions. This study provides a theoretical foundation and groundwork for future research on the functions and mechanisms of cassava *DIR* genes in plant growth and development.

Supplementary Materials: The following supporting information can be downloaded at: <https://www.mdpi.com/article/10.3390/agronomy14081758/s1>, Figure S1: The expression profiles of *MeDIR* genes profile cassava were infected with *Xam668* for 8, 24, and 50 h. Log₂ transformed FPKM value was used to create the heat map. The scale represents the relative signal intensity of FPKM values; Figure S2: The expression of *MeDIR* gene profile in cassava leaves and roots was observed after 7 and 14 d of atrazine stress. Control roots (RC_7d, RC_14d) and leaves (LC_7d, LC_14d). Treatment roots (RT_7d, RT_14d) and leaves (LT_7d, LT_14d). Log₂ FC value was used to create the heat map. Red indicates that the gene is up-regulated, blue indicates that the gene is down-regulated, and gray indicates that the gene has no Log₂ FC value in the differential comparison group; Figure S3: The expression of *MeDIR* gene profile of cassava was observed after 10 μM and 100 μM CdCl₂ stress for 48 h. 0 μM (CK), 10 μM (T10), and 100 μM (T100). Log₂ FC value was used to create the heat map. Red indicates that the gene is up-regulated, blue indicates that the gene is down-regulated, and gray indicates that the gene has no Log₂ FC value in the differential comparison group; Table S1: The primer was designed for qRT-PCR; Table S2: Basic information of *DIR* genes in cassava; Table S3: The sequence relatedness of *MeDIRs*; Table S4: The secondary structure of *MeDIR* protein sequences; Table S5: The probability and identity of homologous relationships of *MeDIRs*; Table S6: Segmental duplications of *MeDIR* genes and Ka/Ks ratio analysis; Table S7: The function and number of *cis*-acting regulatory elements in the promoter regions of *MeDIR* genes; Table S8: Functional annotation (gene ontology) of *MeDIR* proteins; Table S9: Detailed situation table of expression quantity values in Figures 8 and S1 and Log₂FC values in Figures S2 and S3.

Author Contributions: Conceptualization, R.Z. and S.F.; methodology, M.L. (Mingchao Li), K.L., W.Z., M.L. (Man Liu) and H.H.; software, M.L. (Mingchao Li) and K.L.; validation, M.L. (Mingchao Li), W.Z. and M.L. (Man Liu); formal analysis, M.L. (Mingchao Li); investigation, M.L. (Mingchao Li), W.Z., M.L. (Man Liu), H.H. and Y.Z.; visualization, W.Z., M.L. (Man Liu) and H.H.; literature search, M.L. (Man Liu) and H.H.; figures, W.Z.; writing—original draft preparation, M.L. (Mingchao Li) and K.L.; writing—review and editing, M.L. (Mingchao Li), K.L., Y.Z., Y.C., S.F. and R.Z. All authors have read and agreed to the published version of the manuscript.

Funding: This research was funded by the National Natural Science Foundation of China (No: 32160324, 42005138) and the China Agriculture Research System (No. CARS-11-hncyh).

Data Availability Statement: The original data presented in the study are openly available in NCBI at <https://www.ncbi.nlm.nih.gov/> (accessed on 1 July 2024), reference numbers PRJNA324539, PRJNA163523, PRJNA1128429, and PRJNA1127687; [PRJNA324539] [<https://www.ncbi.nlm.nih.gov/bioproject/?term=PRJNA324539>, accessed on 7 July 2024]. [PRJNA163523] [<https://www.ncbi>

[nlm.nih.gov/bioproject/?term=PRJNA163523](https://www.ncbi.nlm.nih.gov/bioproject/?term=PRJNA163523), accessed on 7 July 2024]. [PRJNA1128429] [<https://www.ncbi.nlm.nih.gov/bioproject/?term=PRJNA1128429>, accessed on 7 July 2024]. [PRJNA1127687] [<https://www.ncbi.nlm.nih.gov/bioproject/?term=PRJNA1127687>, accessed on 7 July 2024].

Conflicts of Interest: The authors declare no conflicts of interest.

Abbreviations

Abbreviation	Full name
ABA	abscisic acid
AOC	allene oxide cyclase-like protein
BP	biological process
CA	coniferyl alcohol
CaCl ₂	cadmium chloride
CC	cellular component
CDD	Conserved Domain Database
CDs	coding DNA sequences
CPR	Novo Nordisk Foundation Center for Protein Research
DIR	dirigent
drr206	disease resistance response protein 206
EGTA	ethylene glycol tetraacetic acid
EMBL-EBI	European Bioinformatics Institute
FEC	friable embryogenic callus
FPKM	transcript per million reads mapped
FR	fibrous root
GO	gene ontology
GRAVY	grand average of hydropathicity
HMM	Hidden Markov Model
Ka	non-synonymous substitution rate
Ks	synonymous substitution rate
log ₂ FC	log ₂ Fold Change
MF	molecular function
MW	molecular weight
NaCl	sodium chloride
NJ	neighbor-joining
OES	organized embryogenic structures
PDD	postharvest physiological deterioration
PEG	polyethylene glycol
pI	isoelectric point
PIR	Protein Information Resource
qRT-PCR	quantitative real-time PCR
RAM	root apical meristem
SAM	shoot apical meristem
SC9	South China 9
SR	storage root

References

- Ralph, S.; Park, J.Y.; Bohlmann, J.; Mansfield, S.D. Dirigent proteins in conifer defense: Gene discovery, phylogeny, and differential wound- and insect-induced expression of a family of *DIR* and *DIR-like* genes in spruce (*Picea* spp.). *Plant Mol. Biol.* **2006**, *60*, 21–40. [[CrossRef](#)]
- Davin, L.B.; Wang, H.B.; Crowell, A.L.; Bedgar, D.L.; Martin, D.M.; Sarkanen, S.; Lewis, N.G. Stereoselective bimolecular phenoxyl radical coupling by an auxiliary (dirigent) protein without an active center. *Science* **1997**, *275*, 362–366. [[CrossRef](#)] [[PubMed](#)]
- Davin, L.B.; Lewis, N.G. Lignin primary structures and dirigent sites. *Curr. Opin. Biotechnol.* **2005**, *16*, 407–415. [[CrossRef](#)] [[PubMed](#)]
- Satake, H.; Koyama, T.; Bahabadi, S.E.; Matsumoto, E.; Ono, E.; Murata, J. Essences in metabolic engineering of lignan biosynthesis. *Metabolites* **2015**, *5*, 270–290. [[CrossRef](#)]
- Burlat, V.; Kwon, M.; Davin, L.B.; Lewis, N.G. Dirigent proteins and dirigent sites in lignifying tissues. *Phytochemistry* **2001**, *57*, 883–897. [[CrossRef](#)] [[PubMed](#)]

6. Vanholme, R.; Morreel, K.; Darrach, C.; Oyarce, P.; Grabber, J.H.; Ralph, J.; Boerjan, W. Metabolic engineering of novel lignin in biomass crops. *New Phytol.* **2012**, *196*, 978–1000. [[CrossRef](#)] [[PubMed](#)]
7. Barros, J.; Serk, H.; Granlund, I.; Pesquet, E. The cell biology of lignification in higher plants. *Ann. Bot.* **2015**, *115*, 1053–1074. [[CrossRef](#)]
8. Paniagua, C.; Bilkova, A.; Jackson, P.; Dabravolski, S.; Riber, W.; Didi, V.; Houser, J.; Gigli-Bisceglia, N.; Wimmerova, M.; Budínská, E.; et al. Dirigent proteins in plants: Modulating cell wall metabolism during abiotic and biotic stress exposure. *J. Exp. Bot.* **2017**, *68*, 3287–3301. [[CrossRef](#)] [[PubMed](#)]
9. Davin, L.B.; Lewis, N.G. Dirigent proteins and dirigent sites explain the mystery of specificity of radical precursor coupling in lignan and lignin biosynthesis. *Plant Physiol.* **2000**, *123*, 453–462. [[CrossRef](#)]
10. Corbin, C.; Drouet, S.; Markulin, L.; Auguin, D.; Lainé, É.; Davin, L.B.; Cort, J.R.; Lewis, N.G.; Hano, C. A genome-wide analysis of the flax (*Linum usitatissimum* L.) dirigent protein family: From gene identification and evolution to differential regulation. *Plant Mol. Biol.* **2018**, *97*, 73–101. [[CrossRef](#)]
11. Ralph, S.G.; Jancsik, S.; Bohlmann, J. Dirigent proteins in conifer defense II: Extended gene discovery, phylogeny, and constitutive and stress-induced gene expression in spruce (*Picea* spp.). *Phytochemistry* **2007**, *68*, 1975–1991. [[CrossRef](#)]
12. Xia, Z.Q.; Costa, M.A.; Proctor, J.; Davin, L.B.; Lewis, N.G. Dirigent-mediated podophyllotoxin biosynthesis in *Linum flavum* and *Podophyllum peltatum*. *Phytochemistry* **2000**, *55*, 537–549. [[CrossRef](#)]
13. Kim, M.K.; Jeon, J.H.; Fujita, M.; Davin, L.B.; Lewis, N.G. The western red cedar (*Thuja plicata*) 8-8' DIRIGENT family displays diverse expression patterns and conserved monolignol coupling specificity. *Plant Mol. Biol.* **2002**, *49*, 199–214. [[CrossRef](#)]
14. Ma, Q.H.; Liu, Y.C. *Tadir13*, a dirigent protein from wheat, promotes lignan biosynthesis and enhances pathogen resistance. *Plant Mol. Biol. Rep.* **2015**, *33*, 143–152. [[CrossRef](#)]
15. Khan, A.; Li, R.J.; Sun, J.T.; Ma, F.; Zhang, H.X.; Jin, J.H.; Ali, M.; Haq, S.U.; Wang, J.E.; Gong, Z.H. Genome-wide analysis of dirigent gene family in pepper (*Capsicum annuum* L.) and characterization of *CaDIR7* in biotic and abiotic stresses. *Sci. Rep.* **2018**, *8*, 5500. [[CrossRef](#)] [[PubMed](#)]
16. Liao, Y.; Liu, S.; Jiang, Y.; Hu, C.; Zhang, X.; Cao, X.; Xu, Z.; Gao, X.; Li, L.; Zhu, J.; et al. Genome-wide analysis and environmental response profiling of dirigent family genes in rice (*Oryza sativa*). *Genes Genom.* **2017**, *39*, 47–62. [[CrossRef](#)]
17. Duan, W.; Xue, B.; He, Y.; Liao, S.; Li, X.; Li, X.; Liang, Y.K. Genome-wide identification and expression pattern analysis of dirigent members in the genus *Oryza*. *Int. J. Mol. Sci.* **2023**, *24*, 7189. [[CrossRef](#)] [[PubMed](#)]
18. Jia, W.; Xiong, Y.; Li, M.; Zhang, S.; Han, Z.; Li, K. Genome-wide identification, characterization, evolution and expression analysis of the *DIR* gene family in potato (*Solanum tuberosum*). *Front. Genet.* **2023**, *14*, 1224015. [[CrossRef](#)]
19. Liu, C.; Qin, Z.; Zhou, X.; Xin, M.; Wang, C.; Liu, D.; Li, S. Expression and functional analysis of the Propamocarb-related gene *CsDIR16* in cucumbers. *BMC Plant Biol.* **2018**, *18*, 16. [[CrossRef](#)]
20. Effenberger, I.; Harport, M.; Pfannstiel, J.; Klaiber, I.; Schaller, A. Expression in *Pichia pastoris* and characterization of two novel dirigent proteins for atropselective formation of gossypol. *Appl. Microbiol. Biotechnol.* **2017**, *101*, 2021–2032. [[CrossRef](#)]
21. Uchida, K.; Akashi, T.; Aoki, T. The missing link in leguminous pterocarpan biosynthesis is a dirigent domain-containing protein with isoflavanol dehydratase activity. *Plant Cell Physiol.* **2017**, *58*, 398–408. [[CrossRef](#)] [[PubMed](#)]
22. Meng, Q.; Moinuddin, S.G.A.; Kim, S.J.; Bedgar, D.L.; Costa, M.A.; Thomas, D.G.; Young, R.P.; Smith, C.A.; Cort, J.R.; Davin, L.B.; et al. Pterocarpan synthase (PTS) structures suggest a common quinone methide-stabilizing function in dirigent proteins and proteins with dirigent-like domains. *J. Biol. Chem.* **2020**, *295*, 11584–11601. [[CrossRef](#)]
23. Hosmani, P.S.; Kamiya, T.; Danku, J.; Naseer, S.; Geldner, N.; Guerinot, M.L.; Salt, D.E. Dirigent domain-containing protein is part of the machinery required for formation of the lignin-based Casparian strip in the root. *Proc. Natl. Acad. Sci. USA* **2013**, *110*, 14498–14503. [[CrossRef](#)]
24. Wu, R.; Wang, L.; Wang, Z.; Shang, H.; Liu, X.; Zhu, Y.; Qi, D.; Deng, X. Cloning and expression analysis of a dirigent protein gene from the resurrection plant *Boea hygrometrica*. *Prog. Nat. Sci.* **2009**, *19*, 347–352. [[CrossRef](#)]
25. Xue, B.; Duan, W.; Gong, L.; Zhu, D.; Li, X.; Li, X.; Liang, Y.K. The *OsDIR55* gene increases salt tolerance by altering the root diffusion barrier. *Plant J.* **2024**, *118*, 1550–1568. [[CrossRef](#)]
26. Xu, W.; Liu, T.; Zhang, H.; Zhu, H. Mungbean *DIRIGENT* Gene subfamilies and their expression profiles under salt and drought stresses. *Front. Genet.* **2021**, *12*, 658148. [[CrossRef](#)]
27. Zhou, J.; Lee, C.; Zhong, R.; Ye, Z.H. *MYB58* and *MYB63* are transcriptional activators of the lignin biosynthetic pathway during secondary cell wall formation in Arabidopsis. *Plant Cell* **2009**, *21*, 248–266. [[CrossRef](#)] [[PubMed](#)]
28. Wang, Y.; Fristensky, B.J.M.B. Transgenic canola lines expressing pea defense gene DRR206 have resistance to aggressive blackleg isolates and to *Rhizoctonia solani*. *Mol. Breed.* **2001**, *8*, 263–271. [[CrossRef](#)]
29. Shi, H.; Liu, Z.; Zhu, L.; Zhang, C.; Chen, Y.; Zhou, Y.; Li, F.; Li, X. Overexpression of cotton (*Gossypium hirsutum*) dirigent1 gene enhances lignification that blocks the spread of *Verticillium dahliae*. *Acta Biochim. Biophys. Sin.* **2012**, *44*, 555–564. [[CrossRef](#)]
30. Li, N.; Zhao, M.; Liu, T.; Dong, L.; Cheng, Q.; Wu, J.; Wang, L.; Chen, X.; Zhang, C.; Lu, W.; et al. A novel soybean dirigent gene *GmDIR22* contributes to promotion of lignan biosynthesis and enhances resistance to *Phytophthora sojae*. *Front. Plant Sci.* **2017**, *8*, 1185. [[CrossRef](#)]
31. Taylor, N.; Chavarriaga, P.; Raemakers, K.; Siritunga, D.; Zhang, P. Development and application of transgenic technologies in cassava. *Plant Mol. Biol.* **2004**, *56*, 671–688. [[CrossRef](#)] [[PubMed](#)]

32. Li, M.; Zi, X.; Tang, J.; Zhou, H.; Cai, Y. Silage fermentation, chemical composition and ruminal degradation of king grass, cassava foliage and their mixture. *Grassland Sci.* **2019**, *64*, 210–215. [[CrossRef](#)]
33. Li, M.; Zi, X.J.; Diao, Q.Y.; Hu, H.C.; Tang, J.; Zhou, H.L. Effect of tannic acids on the fermentation quality and aerobic stability of cassava foliage. *Pratacult. Sci.* **2019**, *36*, 1662–1667.
34. Li, S.; Cui, Y.; Zhou, Y.; Luo, Z.; Liu, J.; Zhao, M. The industrial applications of cassava: Current status, opportunities and prospects. *J. Sci. Food Agric.* **2017**, *97*, 2282–2290. [[CrossRef](#)] [[PubMed](#)]
35. Mohidin, S.R.N.S.P.; Moshawih, S.; Hermansyah, A.; Asmuni, M.I.; Shafqat, N.; Ming, L.C. Cassava (*Manihot esculenta* Crantz): A systematic review for the pharmacological activities, traditional uses, nutritional values, and phytochemistry. *J. Evid. Based Integr. Med.* **2023**, *28*, 2515690X231206227. [[CrossRef](#)] [[PubMed](#)]
36. Mistry, J.; Chuguransky, S.; Williams, L.; Qureshi, M.; Salazar, G.A.; Sonnhammer, E.L.L.; Tosatto, S.C.E.; Paladin, L.; Raj, S.; Richardson, L.J.; et al. Pfam: The protein families database in 2021. *Nucleic Acids Res.* **2021**, *49*, D412–D419. [[CrossRef](#)] [[PubMed](#)]
37. Li, M.; Zhang, L.; Zhang, Q.; Zi, X.; Lv, R.; Tang, J.; Zhou, H. Impacts of citric acid and malic acid on fermentation quality and bacterial community of cassava foliage silage. *Front. Microbiol.* **2020**, *11*, 595622. [[CrossRef](#)]
38. Chen, C.; Chen, H.; Zhang, Y.; Thomas, H.R.; Frank, M.H.; He, Y.; Xia, R. TBtools: An integrative toolkit developed for interactive analyses of big biological data. *Mol. Plant* **2020**, *13*, 1194–1202. [[CrossRef](#)] [[PubMed](#)]
39. Marchler-Bauer, A.; Bo, Y.; Han, L.; He, J.; Lanczycki, C.J.; Lu, S.; Chitsaz, F.; Derbyshire, M.K.; Geer, R.C.; Gonzales, N.R.; et al. CDD/SPARCLE: Functional classification of proteins via subfamily domain architectures. *Nucleic Acids Res.* **2017**, *45*, D200–D203. [[CrossRef](#)] [[PubMed](#)]
40. McDowall, J.; Hunter, S. InterPro protein classification. *Methods Mol. Biol.* **2011**, *694*, 37–47. [[CrossRef](#)] [[PubMed](#)]
41. Gasteiger, E.; Gattiker, A.; Hoogland, C.; Ivanyi, I.; Appel, R.D.; Bairoch, A. ExPASy: The proteomics server for in-depth protein knowledge and analysis. *Nucleic Acids Res.* **2003**, *31*, 3784–3788. [[CrossRef](#)] [[PubMed](#)]
42. Horton, P.; Park, K.J.; Obayashi, T.; Fujita, N.; Harada, H.; Adams-Collier, C.J.; Nakai, K. WoLF PSORT: Protein localization predictor. *Nucleic Acids Res.* **2007**, *35*, W585–W587. [[CrossRef](#)] [[PubMed](#)]
43. Guo, A.Y.; Zhu, Q.H.; Chen, X.; Luo, J.C. [GSDS: A gene structure display server]. *Yi Chuan* **2007**, *29*, 1023–1026. [[CrossRef](#)] [[PubMed](#)]
44. Crooks, G.E.; Hon, G.; Chandonia, J.M.; Brenner, S.E. WebLogo: A sequence logo generator. *Genome Res.* **2004**, *14*, 1188–1189. [[CrossRef](#)] [[PubMed](#)]
45. Larkin, M.A.; Blackshields, G.; Brown, N.P.; Chenna, R.; McGettigan, P.A.; McWilliam, H.; Valentin, F.; Wallace, I.M.; Wilm, A.; Lopez, R.; et al. Clustal W and Clustal X version 2.0. *Bioinformatics.* **2007**, *23*, 2947–2948. [[CrossRef](#)] [[PubMed](#)]
46. Zhang, H.; Gao, S.; Lercher, M.J.; Hu, S.; Chen, W.H. EvolView, an online tool for visualizing, annotating and managing phylogenetic trees. *Nucleic Acids Res.* **2012**, *40*, W569–W572. [[CrossRef](#)]
47. Wang, Y.; Tang, H.; Debarry, J.D.; Tan, X.; Li, J.; Wang, X.; Lee, T.H.; Jin, H.; Marler, B.; Guo, H.; et al. MCScanX: A toolkit for detection and evolutionary analysis of gene synteny and collinearity. *Nucleic Acids Res.* **2012**, *40*, e49. [[CrossRef](#)]
48. Lescot, M.; Déhais, P.; Thijs, G.; Marchal, K.; Moreau, Y.; Vande Peer, Y.; Rouzé, P.; Rombauts, S. PlantCARE, a database of plant *cis*-acting regulatory elements and a portal to tools for in silico analysis of promoter sequences. *Nucleic Acids Res.* **2002**, *30*, 325–327. [[CrossRef](#)]
49. Franceschini, A.; Szklarczyk, D.; Frankild, S.; Kuhn, M.; Simonovic, M.; Roth, A.; Lin, J.; Minguez, P.; Bork, P.; von Mering, C.; et al. STRING v9.1: Protein-protein interaction networks, with increased coverage and integration. *Nucleic Acids Res.* **2013**, *41*, D808–D815. [[CrossRef](#)]
50. Szklarczyk, D.; Franceschini, A.; Wyder, S.; Forslund, K.; Heller, D.; Huerta-Cepas, J.; Simonovic, M.; Roth, A.; Santos, A.; Tsafou, K.P.; et al. STRING v10: Protein-protein interaction networks, integrated over the tree of life. *Nucleic Acids Res.* **2015**, *43*, D447–D452. [[CrossRef](#)]
51. Wilson, M.C.; Mutka, A.M.; Hummel, A.W.; Berry, J.; Chauhan, R.D.; Vijayaraghavan, A.; Taylor, N.J.; Voytas, D.F.; Chitwood, D.H.; Bart, R.S. Gene expression atlas for the food security crop cassava. *New Phytol.* **2017**, *213*, 1632–1641. [[CrossRef](#)]
52. Bart, R.; Cohn, M.; Kassen, A.; McCallum, E.J.; Shybut, M.; Petriello, A.; Krasileva, K.; Dahlbeck, D.; Medina, C.; Alicai, T.; et al. High-throughput genomic sequencing of cassava bacterial blight strains identifies conserved effectors to target for durable resistance. *Proc. Natl. Acad. Sci. USA* **2012**, *109*, E1972–E1979. [[CrossRef](#)]
53. Huang, H.; Song, J.; Feng, Y.; Zheng, L.; Chen, Y.; Luo, K. Genome-wide identification and expression analysis of the *SHI*-related sequence family in cassava. *Genes* **2023**, *14*, 870. [[CrossRef](#)]
54. Zheng, L.; Wan, Q.; Wang, H.; Guo, C.; Niu, X.; Zhang, X.; Zhang, R.; Chen, Y.; Luo, K. Genome-wide identification and expression of *TIFY* family in cassava (*Manihot esculenta* Crantz). *Front. Plant Sci.* **2022**, *13*, 1017840. [[CrossRef](#)] [[PubMed](#)]
55. Cao, M.; Zheng, L.; Li, J.; Mao, Y.; Zhang, R.; Niu, X.; Geng, M.; Zhang, X.; Huang, W.; Luo, K.; et al. Transcriptomic profiling suggests candidate molecular responses to waterlogging in cassava. *PLoS ONE* **2022**, *17*, e0261086. [[CrossRef](#)]
56. Schmittgen, T.D.; Livak, K.J. Analyzing real-time PCR data by the comparative C(T) method. *Nat. Protoc.* **2008**, *3*, 1101–1108. [[CrossRef](#)] [[PubMed](#)]
57. Ma, X.; Xu, W.; Liu, T.; Chen, R.; Zhu, H.; Zhang, H.; Cai, C.; Li, S. Functional characterization of soybean (*Glycine max*) *DIRIGENT* genes reveals an important role of *GmDIR27* in the regulation of pod dehiscence. *Genomics* **2021**, *113*, 979–990. [[CrossRef](#)] [[PubMed](#)]

58. An, F.; Xue, J.; Luo, X.; Chen, T.; Wei, Z.; Zhu, W.; Ou, W.; Li, K.; Cai, J.; Chen, S. *MePOD12* participates the regulation to postharvest physiological deterioration by ROS scavenging and lignin accumulation in cassava tuberous roots. *Postharvest Biol. Technol.* **2024**, *207*, 112609. [[CrossRef](#)]
59. Yan, Y.; Wang, P.; Lu, Y.; Bai, Y.; Wei, Y.; Liu, G.; Shi, H. *MeRAV5* promotes drought stress resistance in cassava by modulating hydrogen peroxide and lignin accumulation. *Plant J.* **2021**, *107*, 847–860. [[CrossRef](#)]
60. Yao, X.; Liang, X.; Chen, Q.; Liu, Y.; Wu, C.; Wu, M.; Shui, J.; Qiao, Y.; Zhang, Y.; Geng, Y. *MePAL6* regulates lignin accumulation to shape cassava resistance against two-spotted spider mite. *Front. Plant Sci.* **2023**, *13*, 1067695. [[CrossRef](#)]
61. Song, M.; Peng, X. Genome-wide identification and characterization of *DIR* genes in *Medicago truncatula*. *Biochem. Genet.* **2019**, *57*, 487–506. [[CrossRef](#)] [[PubMed](#)]
62. Xiong, R.; Peng, Z.; Zhou, H.; Xue, G.; He, A.; Yao, X.; Weng, W.; Wu, W.; Ma, C.; Bai, Q.; et al. Genome-wide identification, structural characterization and gene expression analysis of the WRKY transcription factor family in pea (*Pisum sativum* L.). *BMC Plant Biol.* **2024**, *24*, 113. [[CrossRef](#)]
63. Bai, Y.; Meng, Y.; Huang, D.; Qi, Y.; Chen, M. Origin and evolutionary analysis of the plant-specific TIFY transcription factor family. *Genomics* **2011**, *98*, 128–136. [[CrossRef](#)] [[PubMed](#)]
64. Cai, Z.; Chen, Y.; Liao, J.; Wang, D. Genome-wide identification and expression analysis of jasmonate ZIM domain gene family in tuber mustard (*Brassica juncea* var. *tumida*). *PLoS ONE* **2020**, *15*, e0234738. [[CrossRef](#)] [[PubMed](#)]
65. Liu, C.; Zhang, Q.; Zhu, H.; Cai, C.; Li, S. Characterization of mungbean *CONSTANS-LIKE* genes and functional analysis of *CONSTANS-LIKE 2* in the regulation of flowering time in Arabidopsis. *Front. Plant Sci.* **2021**, *12*, 608603. [[CrossRef](#)] [[PubMed](#)]
66. Luo, R.; Pan, W.; Liu, W.; Tian, Y.; Zeng, Y.; Li, Y.; Li, Z.; Cui, L. The barley *DIR* gene family: An expanded gene family that is involved in stress responses. *Front. Genet.* **2022**, *13*, 1042772. [[CrossRef](#)] [[PubMed](#)]
67. Zhang, K.J.; Xing, W.J.; Sheng, S.A.; Yang, D.K.; Zhen, F.X.; Jiang, H.K.; Yan, C.; Jia, L. Genome-wide identification and expression analysis of eggplant *DIR* gene family in response to biotic and abiotic stresses. *Horticulturae* **2022**, *8*, 732. [[CrossRef](#)]
68. Shi, Y.; Shen, Y.; Ahmad, B.; Yao, L.; He, T.; Fan, J.; Liu, Y.; Chen, Q.; Wen, Z. Genome-wide identification and expression analysis of dirigent gene family in strawberry (*Fragaria vesca*) and functional characterization of *FvDIR13*. *Sci. Hortic.* **2022**, *297*, 110913. [[CrossRef](#)]
69. Yadav, V.; Wang, Z.; Yang, X.; Wei, C.; Changqing, X.; Zhang, X. Comparative analysis, characterization and evolutionary study of dirigent gene Family in cucurbitaceae and expression of novel dirigent peptide against powdery mildew stress. *Genes.* **2021**, *12*, 326. [[CrossRef](#)] [[PubMed](#)]
70. Cheng, X.; Su, X.; Muhammad, A.; Li, M.; Zhang, J.; Sun, Y.; Li, G.; Jin, Q.; Cai, Y.; Lin, Y. Molecular characterization, evolution, and expression profiling of the Dirigent (*DIR*) family genes in chinese white pear (*Pyrus bretschneideri*). *Front. Genet.* **2018**, *9*, 136. [[CrossRef](#)]
71. Jiang, S.Y.; González, J.M.; Ramachandran, S. Comparative genomic and transcriptomic analysis of tandemly and segmentally duplicated genes in rice. *PLoS ONE* **2013**, *8*, e63551. [[CrossRef](#)]
72. Cannon, S.B.; Mitra, A.; Baumgarten, A.; Young, N.D.; May, G. The roles of segmental and tandem gene duplication in the evolution of large gene families in *Arabidopsis thaliana*. *BMC Plant Biol.* **2004**, *4*, 10. [[CrossRef](#)] [[PubMed](#)]
73. Zhu, D.; Li, R.; Liu, X.; Sun, M.; Wu, J.; Zhang, N.; Zhu, Y. The positive regulatory roles of the TIFY10 proteins in plant responses to alkaline stress. *PLoS ONE* **2014**, *9*, e111984. [[CrossRef](#)]
74. Hernandez-Garcia, C.M.; Finer, J.J. Identification and validation of promoters and *cis*-acting regulatory elements. *Plant Sci.* **2014**, *217–218*, 109–119. [[CrossRef](#)] [[PubMed](#)]
75. Noman, A.; Kanwal, H.; Khalid, N.; Sanaullah, T.; Tufail, A.; Masood, A.; Sabir, S.U.; Aqeel, M.; He, S. Perspective research progress in cold responses of *capsella bursa-pastoris*. *Front. Plant Sci.* **2017**, *8*, 1388. [[CrossRef](#)]
76. Heidari, P.; Ahmadzadeh, M.; Izanlo, F.; Nussbaumer, T. In silico study of the *CESA* and *CSL* gene family in *Arabidopsis thaliana* and *Oryza sativa*: Focus on post-translation modifications. *Plant Gene* **2019**, *19*, 100189. [[CrossRef](#)]
77. Yang, X.; Zhong, S.; Zhang, Q.; Ren, Y.; Sun, C.; Chen, F. A loss-of-function of the dirigent gene *TaDIR-B1* improves resistance to *Fusarium crown rot* in wheat. *Plant Biotechnol. J.* **2021**, *19*, 866–868. [[CrossRef](#)] [[PubMed](#)]
78. Moerschbacher, B.M.; Noll, U.; Gorrichon, L.; Reisener, H.J. Specific inhibition of lignification breaks hypersensitive resistance of wheat to stem rust. *Plant Physiol.* **1990**, *93*, 465–470. [[CrossRef](#)]
79. Wang, Z.; Zhang, B.; Chen, Z.; Wu, M.; Chao, D.; Wei, Q.; Xin, Y.; Li, L.; Ming, Z.; Xia, J. Three *OsMYB36* members redundantly regulate casparian strip formation at the root endodermis. *Plant Cell* **2022**, *34*, 2948–2968. [[CrossRef](#)]
80. Guo, W.L.; Chen, R.G.; Gong, Z.H.; Yin, Y.X.; Ahmed, S.S.; He, Y.M. Exogenous abscisic acid increases antioxidant enzymes and related gene expression in pepper (*Capsicum annuum*) leaves subjected to chilling stress. *Genet. Mol. Res.* **2012**, *11*, 4063–4080. [[CrossRef](#)]
81. Gong, L.; Li, B.; Zhu, T.; Xue, B. Genome-wide identification and expression profiling analysis of *DIR* gene family in *Setaria italica*. *Front. Plant Sci.* **2023**, *14*, 1243806. [[CrossRef](#)] [[PubMed](#)]
82. Fujita, Y.; Yoshida, T.; Yamaguchi-Shinozaki, K. Pivotal role of the AREB/ABF-SnRK2 pathway in ABRE-mediated transcription in response to osmotic stress in plants. *Physiol. Plant.* **2013**, *147*, 15–27. [[CrossRef](#)] [[PubMed](#)]

Disclaimer/Publisher’s Note: The statements, opinions and data contained in all publications are solely those of the individual author(s) and contributor(s) and not of MDPI and/or the editor(s). MDPI and/or the editor(s) disclaim responsibility for any injury to people or property resulting from any ideas, methods, instructions or products referred to in the content.